crestr An R package to perform probabilistic climate reconstructions from palaeoecological datasets

Manuel Chevalier[1, 2]

[1]Institute of Geosciences, Sect. Meteorology, Rheinische Friedrich-Wilhelms-Universität Bonn, Auf dem Hügel 20, 53121 Bonn, Germany
[2]Institute of Earth Surface Dynamics, Geopolis, University of Lausanne, Lausanne, Switzerland

Correspondence: Manuel Chevalier (chevalier.manuel@gmail.com)

Abstract. Statistical climate reconstruction techniques are fundamental tools to study past climate variability from fossil proxy data. In particular, the methods based on probability density functions (or PDFs) can be used in various environments and with different climate proxies because they rely on elementary calibration data (*i.e.* modern geolocalised presence data). However, the difficulty of accessing and curating these calibration data and the complexity of interpreting probabilistic results have often limited their use in palaeoclimatological studies. Here, I introduce a new R package (*crestr*) to apply the PDF-based method CREST (Climate REconstruction SofTware) on diverse palaeoecological datasets and address these problems. *crestr* includes a globally curated calibration dataset for six common climate proxies (*i.e.* plants, beetles, chironomids, rodents, foraminifera, and dinoflagellate cysts) associated with an extensive range of climate variables (20 terrestrial and 19 marine variables) that enables its use in most terrestrial and marine environments. Private data collections can also be used instead of, or in combination with, the provided calibration dataset. The package includes a suite of graphical diagnostic tools to represent the data at each step of the reconstruction process and provide insights into the effect of the different modelling assumptions and external factors that underlie a reconstruction. With this R package, the CREST method can now be used in a scriptable environment and thus be more easily integrated with existing workflows. It is hoped that *crestr* will be used to produce the much-needed quantified climate reconstructions from the many regions where they are currently lacking, despite the availability of suitable fossil records. To support this development, the use of the package is illustrated with a step-by-step replication of a 790,000 year long mean annual temperature reconstruction based on a pollen record from southeastern Africa.

1 Introduction

Fossil-based climate reconstruction techniques are commonly used to quantify past climates and shed light on the nature of the drivers of climate change across space and time. Over the years, numerous techniques of increasing complexity have been proposed, each one based on a unique set of assumptions regarding the modelling of (palaeo)ecological datasets and their translation into climate reconstructions (*e.g.* Birks et al. (2010), Chevalier et al. (2020b)). In particular, many techniques focus on modelling the relationships between proxy assemblages and climate from collections of modern proxy samples. Of these techniques, Weighted-Averaging (WA, ter Braak and van Dame (1989)), Weighted-Averaging Partial Least Square (WA-PLS, ter Braak et al. (1993)), and the Modern Analogue Technique (MAT, Hutson (1978), Overpeck et al. (1985)) have been the

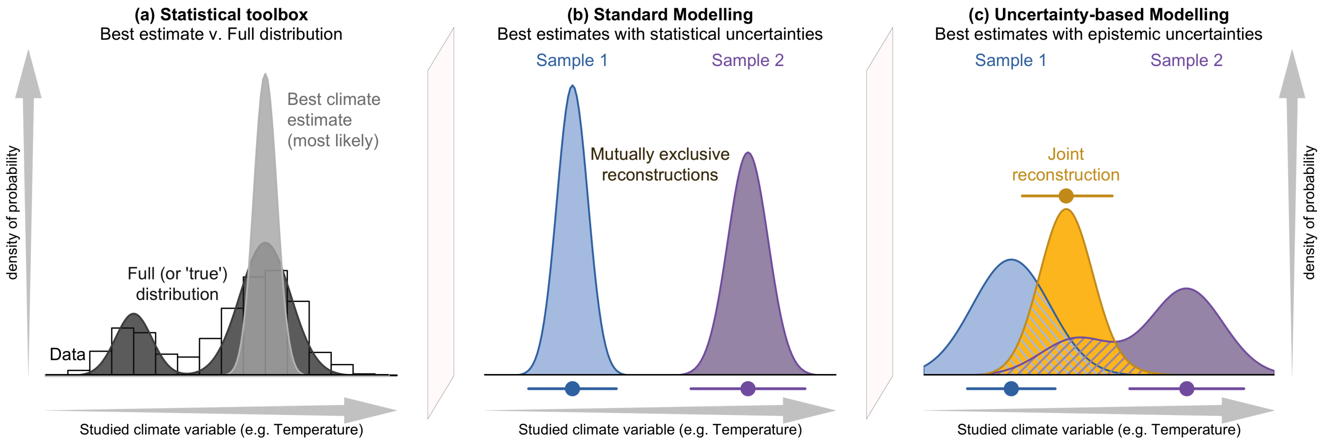
(a) Statistical toolbox
Best estimate v. Full distribution
Best climate estimate (most likely)
Full (or 'true') distribution
Data
density of probability
Studied climate variable (e.g. Temperature)
(b) Standard Modelling
Best estimates with statistical uncertainties
Sample 1
Sample 2
Mutually exclusive reconstructions
Studied climate variable (e.g. Temperature)
(c) Uncertainty-based Modelling
Best estimates with epistemic uncertainties
Sample 1
Sample 2
Joint reconstruction
density of probability
Studied climate variable (e.g. Temperature)

Figure 1. (a) Conceptual illustration of the differences between a modelling approach based on the full spread of the data with the probabilities spread along the climate gradient (e.g. CREST; dark grey), and a modelling approach focused on the estimation of the 'most likely' or 'best' climate value with small statistical errors surrounding it (e.g. MAT or WA-PLS; light grey). In both cases, the area under the curve sums to one. The results of the two types of approaches are illustrated in (b) and (c), where two theoretical fossil assemblages (in blue and purple) are used to produce two independent reconstructions of the same climatic parameter for the same time interval. (b) The two reconstructions are derived from a method that only estimates the most likely climate value, resulting in 'apparently' incompatible reconstructions. (c) The same fossil assemblages are analysed using an approach that estimates their complete uncertainty distributions. In this case, the blue reconstruction is broader, and the purple reconstruction becomes bimodal. When the full spread of these uncertainties is considered, the two reconstructions are not incompatible anymore, and a joint climate estimate (gold) can be derived from their overlapping sections (hashed polygons).

most widely employed because of their conceptual simplicity, their demonstrated capacity to reconstruct climate from various palaeoecological proxies (*e.g.* fossil pollen, chironomids, foraminifera) and their accessibility via multiple software tools. However, the limited availability of the necessary calibration datasets beyond the Northern Hemisphere extratropics has often hindered their application in many environments and regions where quantified climate reconstructions are needed, despite the existence of suitable fossil records (Chevalier et al., 2020b).

In contrast, the 'Indicator species' family of reconstruction techniques uses modern proxy occurrences (*i.e.* collections of locations where the studied proxy species can be observed in modern environments) to estimate individual proxy-climate relationships (Chevalier et al., 2020b). Because such occurrence data are generally easier to obtain than modern proxy assemblages, this fundamental difference implies that Indicator species methods can contribute to filling in the reconstruction gaps that exist at the global scale. The CREST (Climate REconstruction SofTware) technique is a probabilistic Indicator species method initially developed to produce quantified climate reconstructions from southern African pollen records (Chevalier et al., 2014). Derived from the original work of Kühl et al. (2002) —- who first proposed to replace the commonly-used modern proxy assemblages with modern geolocalised occurrence data to estimate probabilistic proxy-climate relationships for palaeoclimatic studies – CREST estimates and combines probabilistic proxy-climate relationships to reconstruct past climate parameters from fossil proxy observations. Built on a private collection of modern plant occurrences held by the South African National

Botanical Institute (SANBI), CREST was first employed to reconstruct diverse temperature, precipitation and moisture-related variables for different time intervals across the southern African drylands (see for instance Chase et al. (2015b), Chase et al. (2015a), Chevalier and Chase (2015), Chevalier and Chase (2016), Lim et al. (2016), Cordova et al. (2017)).

Since the assumptions of CREST do not restrict its use to southern African pollen records, CREST was also integrated into a point-and-click graphical user interface to enable its use by the broader community (Chevalier et al., 2014). However, the complexity of collating and formatting the thousands of distinct occurrences required to estimate reliable proxy-climate relationships limited its practical use. To overcome this limitation, a global, multi-proxy calibration dataset containing millions of modern occurrence data for plants, beetles, chironomids, foraminifera, and diatoms was subsequently released (Chevalier, 2019), and this curated dataset contributed to creating quantified climate reconstructions beyond southern Africa (*e.g.* Yi et al. (2020), Hui et al. (2021), Gibson et al. (2022)). However, maintaining the compatibility of the graphical interface across a range of constantly evolving operating platforms has been challenging. This paper thus introduces a new multi-platform R package *crestr* designed to replace the original interface. *crestr* integrates the global calibration dataset and provides simple solutions to tailor it to the users' specific needs. The package also proposes an array of graphical diagnostic tools to represent the calibration and reconstruction data at different pivotal steps of the reconstruction process and thus facilitate data and result interpretations.

In addition, the advantage of using CREST is not limited to its capacity to produce quantified reconstructions in understudied regions. CREST is equipped with some fundamental statistical features that make it well-adapted to analysing extensive collections of palaeoecological records from any region (Chevalier et al., 2020b). While techniques such as MAT or WA-PLS are primarily designed to associate modern proxy observations with their 'most likely' or 'mean' climate values only, CREST estimates and weighs all the climate values that are compatible with the observed fossil data. As such, the application of CREST yields a probabilistic quantification of all the climate values that are compatible with the studied data instead of simpler, less informative 'most likely' or 'best' climate estimates. While the 'best estimate' approach might be optimal when a fossil assemblage is analysed in complete isolation, the presence of independent - local or regional - information (*e.g.* other reconstructions from the same core or independent records) usually provides additional information that may not always be consistent with the best estimate reconstructions (see Fig. 1). In practice, joint solutions based on all the available information often differ from best climate estimates. Using methods such as CREST that can estimate the full range of climate uncertainties associated with a proxy sample is thus critical to bring reconstructions and even climate simulations together in a cohesive way.

This article introduces the *crestr* R package and provides good-practice recommendations to produce high-quality climate reconstructions. The article is structured as follows: Section 2 summarises the most important mathematics and assumptions underlying the approach. Understanding all the details of this section is not necessary to use the package. Then, Section 3 describes the embedded calibration dataset, how it was built and how the data are structured. Section 4 explains the philosophy and main elements of the package and describes the format of the different input files required. Finally, Section 5 documents a step-by-step guided tour of the package, illustrating the successive stages of a CREST analysis and how to use the diagnostic tools to reproduce a recently published pollen-based temperature reconstruction (Chevalier et al., 2021a).

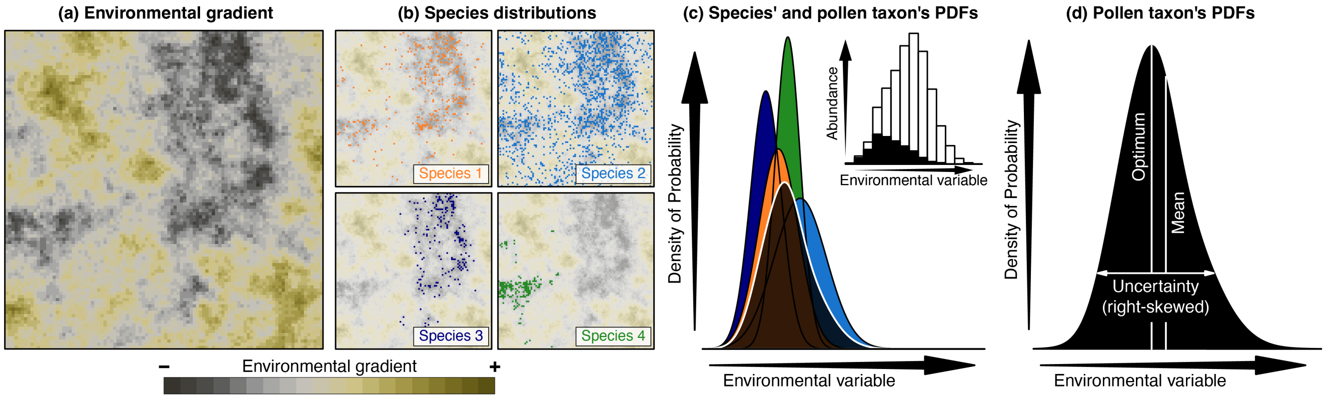

Figure 2. Conceptual representation of CREST illustrated with artificial pollen data. (a) Modern distribution of a climate variable to reconstruct (e.g. temperature). (b) Occurrences of four species part of the same pollen morphotype exhibiting marked preferences for the lowest values of that climate (e.g. dark/cold values) across the study area. (c) Combination of the four species PDFs (in colour) and the resulting pollen taxon PDF (in black). The histogram in the inset panel represents the proportion of the modern climate space (white) occupied by at least one of the four species (black), highlighting the higher chances of observing the taxon at the lower end of the climate gradient. (d) Taxon PDF derived from the combination of the four species PDFs and the type of synthetic statistics (e.g. optimum, mean, uncertainty range) that can be derived from it. While the shape of the species PDFs is constrained, taxon PDFs can be irregular, skewed and even multi-modal.

2 The CREST method

The core process of a CREST reconstruction can be decomposed into two successive stages: 1) modelling the proxy-climate responses of the proxies observed in the fossil sequence by correlating modern occurrence data with corresponding climate values (Fig. 2) and 2) reconstructing past climate by combining these responses based on the information provided by the fossil data. This section presents the most important details of these two stages and details the parameters and modelling assumptions that can be modified in *crestr*. Readers interested in an in-depth description or discussion of the method and its modelling assumptions are referred to Chevalier et al. (2014) and Chevalier et al. (2020b).

2.1 Nature of the required data

Three types of data are required to reconstruct climate parameters with the CREST method:

- A fossil proxy record with several taxa being co-recorded and expressed as counts, percentages or binary presence/absence;
- Modern presence-only occurrence data of species corresponding to the taxa observed in the fossil record (*i.e.* collections of geographical coordinates where the species are observed across a user-defined study area; see Fig. 2b and Section 3 for an example of a curated dataset);
- Climatology(ies) of the variable(s) to reconstruct gridded at the same resolution as the modern occurrences (Fig. 2a). All the climate values observed in the study area define the *climate space*.

2.2 Modelling the proxy-climate relationships

CREST takes into account that some fossil taxa can be identified at the species level (*e.g.* plant macrofossils), while others are only identified at a lower taxonomic resolution (*e.g.* fossil pollen are commonly identified at the genus, sub-family, or even family level; Chevalier et al. (2020b)). The transformation of the information contained in the modern observations of the biological climate proxies into probabilistic climate responses is thus done in one or two steps depending on the taxonomic resolution of the studied proxy. However, determining a list of species that could have produced that fossil is necessary when the observed fossil taxa are not identified at the species level. The way to make this species to fossil proxy association is described in Section 4.3.2.

The individual climate responses of all the species identified are estimated as univariate probability density functions (PDFs) for every climate variable. Because CREST aims to be applicable even in data-sparse environments, the estimation of these responses is based on simple assumptions that exclude using complex algorithms, such as those described in, for instance, the recent review of Valavi et al. (2021). The species' individual responses for climate variable c are derived from the empirical mean ($\overline{m}_{s,c}$) and associated variance ($s^2_{s,c}$) of all the N$_s$ climate values ($c_{s,i}$ where $i = 1, ..., \mathrm{N}_s$) where species s is observed:

$$\overline{m}_{s,c} = \frac{1}{\sum_i k(c_{s,i})} \sum_{i=1}^{\mathrm{N}_s} k(c_{s,i}) c_{s,i} \tag{1}$$

$$s^2_{s,c} = \frac{1}{\sum_i k(c_{s,i})} \sum_{i=1}^{\mathrm{N}_s} k(c_{s,i}) \left(c_{s,i} - \overline{m}^2_{s,c}\right) \tag{2}$$

where $k(c_{s,i})$ is a weighting parameter that can be used to account for the uneven distribution of climate in modern environments (Kühl et al. (2002), Bray et al. (2006)). This correction takes into account that extreme values are usually under-represented in the climate space (see, for instance, the white inset histogram on Fig. 2c), which "pushes" the peak of the PDF$_{\mathrm{sp}}(c, s)$ towards the mean climate observed across the study area (*i.e.* towards the centre of the climate space). It can also artificially shrink the range of the reconstructions. Here, the weights are calculated by first sorting the N climate values that compose the modern climate space into bins of equal width (*e.g.* 2°C or 50 mm). Then, each climate value c_j ($j = 1, ..., \mathrm{N}$) is given a weight $k(c_j)$ defined as the inverse of the number of values that belong to same bin bin$_{c_j}$:

$$k(c_j) = \left(\frac{1}{\mathrm{N}} \sum_{k=1}^{\mathrm{N}} \mathbf{1}_{c_k \in \mathrm{bin}_{c_j}}\right)^{-1} \tag{3}$$

With this correction, the most abundant climate values in the climate space are down-weighted, and the rarer ones are up-weighted so that the distribution of modern climate is overall more 'balanced'. The two parameters $\overline{m}_{s,c}$ and $s_{s,c}$ can be interpreted as the climate preference and tolerance of the species, respectively. For a reliable estimation, excluding species with few observations is recommended. Different studies have shown that a threshold of a minimum of N$_s \geq$ 20-25 distinct occurrences usually leads to reliable estimates (*e.g.* Chevalier et al. (2014), Chevalier et al. (2021a)). However, this number can vary between regions and proxies.

Once estimated, $\overline{m}_{s,c}$ and $s^2_{s,c}$ are used to define a regular, unimodal $\mathrm{PDF}_{\mathrm{sp}}(s,c)$ for species s and climate variable c. Here, we assume that the shape of these species responses should be unimodal and can be either normal:

$$\mathrm{PDF}_{\mathrm{sp}}(s,c) \;=\; \frac{1}{\sqrt{2\pi s^2_{s,c}}}\exp\left(-\frac{(c-\overline{m}_{s,c})^2}{2s^2_{c,s}}\right) \tag{4}$$

or log-normal if the variable is not defined for negative values (*e.g.* precipitation variables):

$$\mathrm{PDF}_{\mathrm{sp}}(s,c) \;=\; \frac{1}{\sqrt{2\pi\sigma^2c^2}}\exp\left(-\frac{(\ln(c)-\mu)^2}{2\sigma^2}\right) \tag{5}$$

$$\text{with}\begin{cases}\mu = \ln(\overline{m}_{s,c}) - \frac{1}{2}\ln\left(1+\frac{s^2_{s,c}}{\overline{m}^2_{s,c}}\right)\\ \sigma^2 = \ln\left(1+\frac{s^2_{s,c}}{\overline{m}^2_{s,c}}\right)\end{cases}$$

For the fossil taxa t that are not identified at the speciel level, the $\mathrm{PDF}_{\mathrm{sp}}(c,s)$ of their $S(t)$ composing species are combined together to meet the taxonomic resolution of the fossil observation (hereafter $\mathrm{PDF}_{\mathrm{tx}}(t,c)$):

$$\mathrm{PDF}_{\mathrm{tx}}(t,c) \;=\; \frac{1}{\sum_s\sqrt{\mathrm{N}_s}}\left(\sum_{s=1}^{S(t)}\sqrt{\mathrm{N}_s}\,\mathrm{PDF}_{\mathrm{sp}}(s,c)\right) \tag{6}$$

This linear combination ensures that all the climate values that support the presence of at least one species have a non-null probability in the $\mathrm{PDF}_{\mathrm{tx}}(t,c)$. Contrary to the previous step, no additional constraints are added here. The distribution of the $\mathrm{PDF}_{\mathrm{tx}}(t,c)$ can thus be asymmetrical and even multimodal if different (groups of) composing species exhibit distinct climate requirements. An additional option is to weigh the different $\mathrm{PDF}_{\mathrm{sp}}(s,c)$ by the square root of the number of individual occurrences composing their distribution (N_s). Considering that it is more difficult to estimate robust parameters with few points, this weighting gives more importance to the species with more extensive geographical distributions today. Said differently, it gives more weight to the species whose climate responses can be the most reliably defined.

Finally, it is important to note that if a fossil taxon is taxonomically resolved at the species level, its number of composing species $S(t)$ equals 1. The resulting $\mathrm{PDF}_{\mathrm{tx}}(t,c)$ is thus equivalent to its $\mathrm{PDF}_{\mathrm{sp}}(s,c)$. A fossil sample can thus be composed of a mix of taxa identified at the species level and taxa identified at a lower taxonomical level without interfering with the reconstruction algorithm.

2.3 Reconstructing climate

Climate c is reconstructed from fossil sample z (itself associated with a unique age, depth or any other identifier) by multiplying the $\mathrm{PDF}_{\mathrm{tx}}(t,c)$ of the $T(z)$ selected taxa:

$$\mathrm{RECON}(c,z) = \left(\prod_{t=1}^{T(z)} \mathrm{PDF}_{\mathrm{tx}}(t,c)^{\omega(t,z)}\right)^{\left(\sum_t \omega(t,z)\right)^{-1}} \quad (7)$$

where $\omega(t,z)$ is a positive value that is used to weigh taxon t in sample z. For presence/absence observations, the weights $\omega(t,z)$ of taxon t will be either one (the taxon is observed) or zero (the taxon is not observed and does not influence the reconstruction). For compositional data, $\omega(t,z)$ can be the observed percentages (*i.e.* values between 0 and 100). However, using raw percentages implies that the observed percentages are directly proportional to the taxa composition across the catchment. This can give considerable weight to abundant, ubiquitous taxa that do not necessarily have a well-defined climate response and, in contrast, can strongly limit the influence of rarer taxa with stricter climate preferences. An empirical normalisation is proposed in CREST to account for the varying production rates, distribution and preservation processes impacting the relative proportions of taxa observed in the sediments (Chevalier et al., 2014). In this taxon-specific scaling method, the percentages of each taxon are divided by their average percentage when it is present (0s are excluded from the calculation of the average):

$$\omega(t,z) = \frac{O(t,z)}{\left(\sum_z O(t,z)\right) \,/\, \left(\sum_z \mathbf{1}_{O(t,z)>0}\right)} \quad (8)$$

where $O(t,z)$ represents the observed percentage of taxon t in sample z. With this transformation, all the normalised percentages vary on a standardised scale. The average presence is given a weight of 1, and values below and above this average presence threshold are assumed to represent lower and higher abundance in the environment, respectively. While the empirical nature of this solution makes it imperfect and sensitive to the quality of the data, it nevertheless enables using percentages to inform the reconstructions. The three weighting options described here are available in *crestr*, but users can also design their own weights to better account for the specificity of their data.

Finally, the presence of each taxon in a sample is considered independent from the others. It is thus possible to select a subset of sensitive taxa to reconstruct a specific climate variable. In some cases, identifying a subgroup of climate-sensitive taxa can help disentangle the different climate signals represented by the palaeoecological data and improve the quality of the reconstructions (Chevalier and Chase, 2015), even if it is not always necessary (Chevalier et al., 2021a). These choices should be dictated by the data themselves and the users' understanding of the studied proxy system. *crestr* provides graphical tools to help identify the possible climate sensitivities of the studied taxa across the study area (Chevalier et al., 2021b).

3 CREST calibration dataset

A multiproxy calibration dataset to estimate PDFs from a global collection of presence-only occurrence data (hereafter proxy 'distributions') was introduced in Chevalier (2019). These data were obtained from the Global Biodiversity Information Facility (GBIF) database, an online collection of geolocalised observations of biological entities (GBIF, 2018). The calibration dataset (hereafter *gbif4crest*, Chevalier, 2020) contains the species distributions of six common palaeoecological fossils: the five taxa presented in the original version of the dataset — plants (GBIF (2020l), GBIF (2020h), GBIF (2020k), GBIF (2020f), GBIF (2020g), GBIF (2020m), GBIF (2020i), GBIF (2020n), GBIF (2020j), GBIF (2021a), GBIF (2021b)) for fossil pollen and macrofossils, chironomids (GBIF, 2020b), beetles (GBIF, 2020a), diatoms (GBIF, 2020c) and foraminifera (GBIF, 2020d) – to which rodents (GBIF, 2020e) were recently added (Fig. 3). These data were curated and stored in a relational database to ensure the consistency of the data.

The coordinates of all the presence records of these six common palaeoecological fossil proxies were mapped onto a grid with a spatial resolution of $0.25 \times 0.25°$ (hereafter QDGC for Quarter-Degree Grid Cell). The QDGC spatial resolution is an empirical trade-off between numerous factors, including the resolution of the presence data, the quality of the data or the spatial representativity of the studied proxy (see discussions in Chevalier et al. (2014) and Chevalier (2019)). However, this trade-off may be suboptimal in some situations. For that reason, *crestr* can also be used with the raw GBIF data (stored in the `DISTRIB` table, Fig. 4) and even independent calibration datasets.

In the *gbif4crest* database, all the QDGC grid cells were associated with a collection of terrestrial and oceanic environmental variables that can be reconstructed (Fick and Hijmans (2017), Zomer et al. (2008), Locarnini et al. (2019), Zweng et al. (2018), Garcia et al. (2019a), Garcia et al. (2019b), Reynolds et al. (2007), see details in Tables 1 and 2). Despite the diversity of variables available, it is recommended to avoid serial reconstructions and, on the contrary, to identify the few important variables for the studied palaeoecological datasets *a priori*. The grid cells were also associated with 'non-reconstructible' environmental and geographical descriptors that serve to tailor the calibration dataset to the users' needs. These include the coordinates, the elevation and elevation variability within the grid cell (Amante and Eakins, 2009), the country (https://www.naturalearthdata.com) or ocean (https://www.marineregions.org) names, as well as different levels of ecological classification for the terrestrial (Olson et al., 2001) and marine (Costello et al., 2017) realms.

In its current version (V2), the *gbif4crest* calibration dataset contains about 25.3 million unique QDGC occurrence data for the six climate proxies. Unfortunately, the density of data available varies between proxies and regions (Fig. 3). Plant data largely dominate the calibration dataset (>22 million unique occurrences) and allow for the use of *crestr* across all landmasses. For the five other proxies, the calibration data are not as extensive. However, these datasets are regularly updated by GBIF. For example, the first version of the gbif4crest dataset released in 2018 contained about 17.5 million QDGC entries (~44% increase). The range of 'reconstructible' areas is thus rapidly broadening (see, for instance, the coverage of Russia by plant data compared to the first version of the *gbif4crest* dataset presented in Chevalier (2019)). This database will be regularly updated, and specific requests can also be made.

The *gbif4crest* database is composed of three main types of data: taxonomic data (`TAXA` table on Fig. 4), distribution data (`DISTRIB` (raw data) and `DISTRIB_QDGC` (curated data) tables) and diverse geopolitical, climatological, and environmental data (`DATA_QDGC` table). Its structure is slightly different from the first version presented in Chevalier (2019), with a grouping of all the separate QDGC tables in a unique `DATA_QDGC` table to enable faster data extraction. The `DISTRIB_QDGC` tables link the `TAXA` and `DATA_QDGC` tables using the unique identifiers `taxonID` and `locID`, respectively. Each occurrence's first and last observation dates are also now included, along with the type of observation reported by GBIF (see https://rs.gbif.org/vocabulary/dwc/basis_of_record.xml) and the number of observations `n_occ` reported between the first and

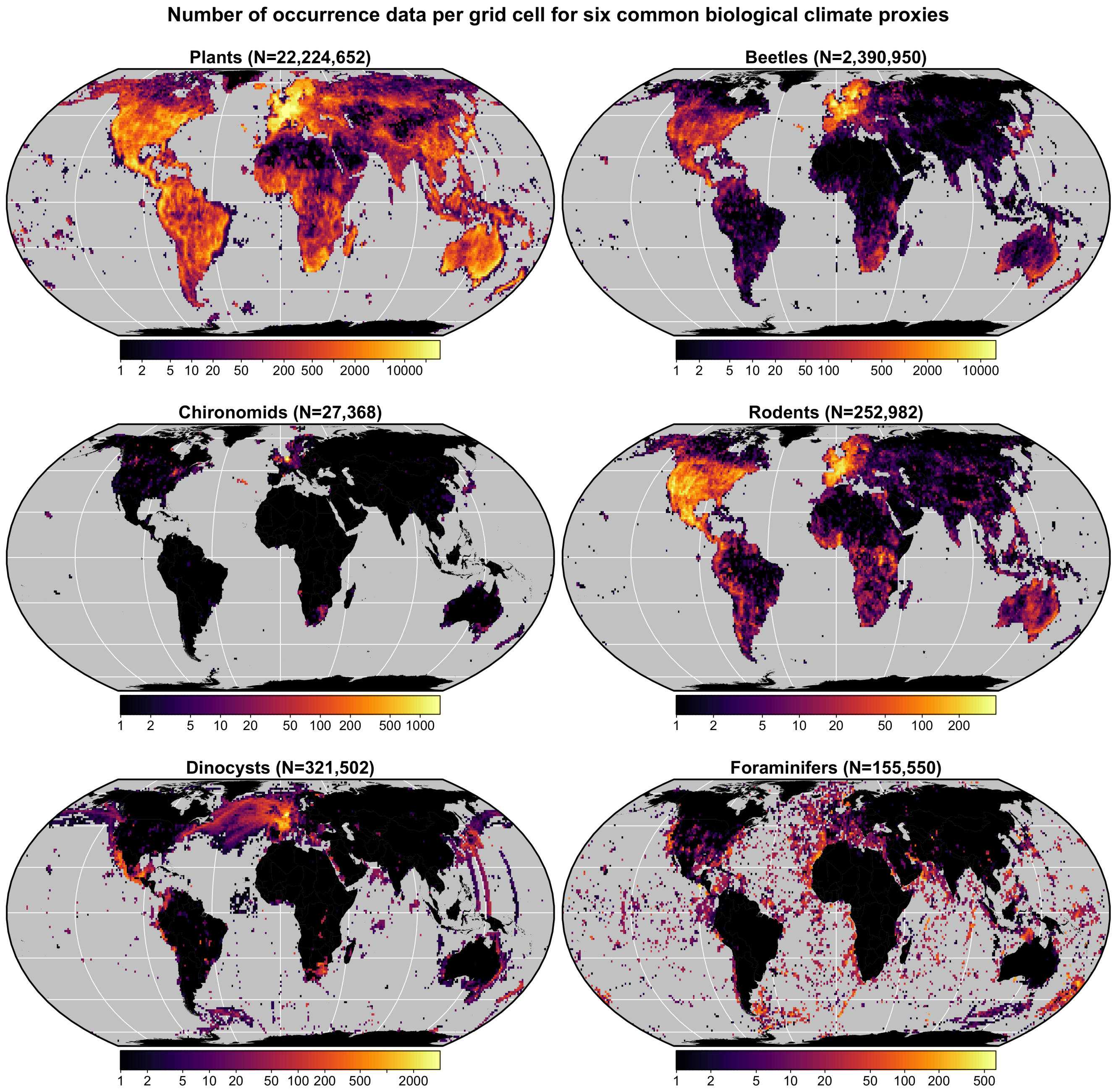

Figure 3. Distribution and grid cell density of the six climate proxies available in the gbif4crest calibration database. The total number of unique species occurrences (N) is indicated for each proxy. The maps are based on the 'Equal Earth' map projection to better account for the relative sizes of the different continents.

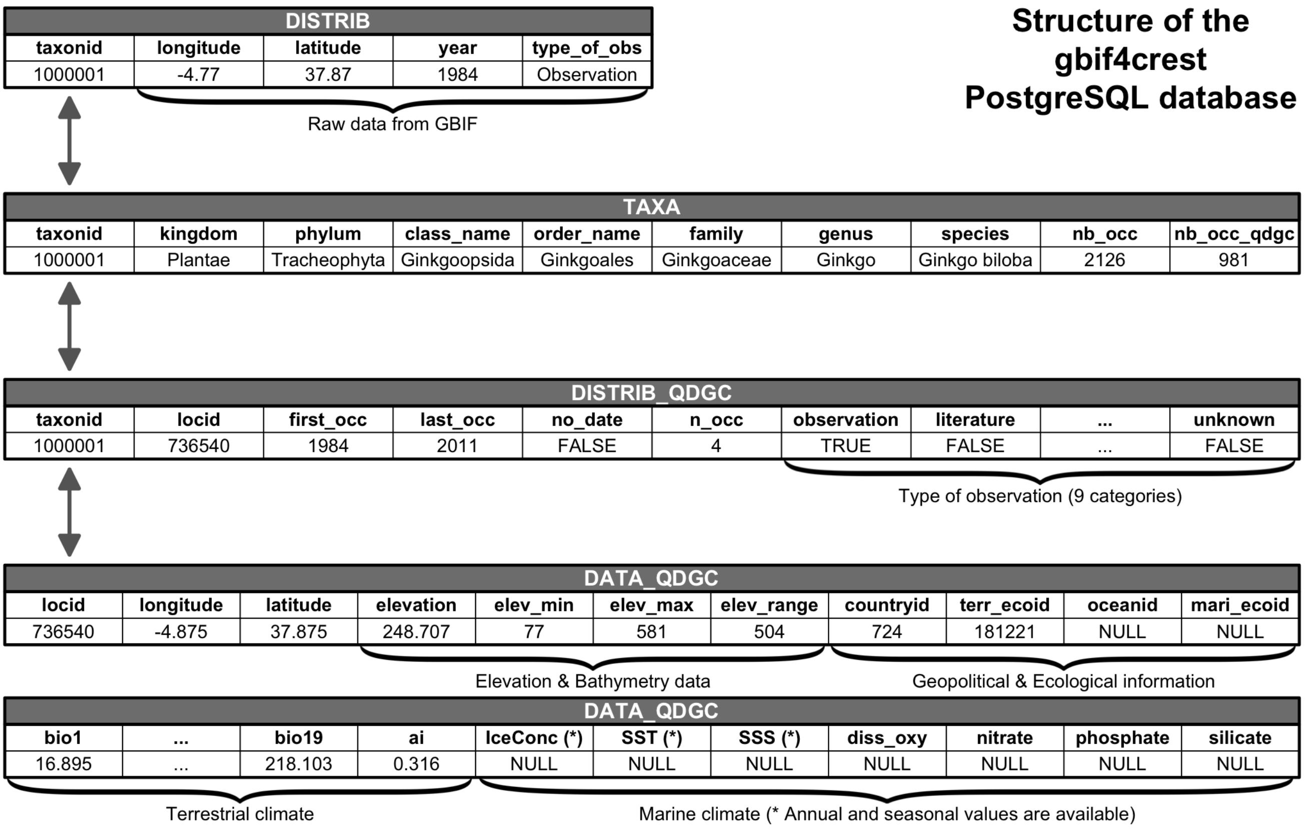

DISTRIB

taxonid	longitude	latitude	year	type_of_obs
1000001	-4.77	37.87	1984	Observation

TAXA

taxonid	kingdom	phylum	class_name	order_name	family	genus	species	nb_occ	nb_occ_qdgc
1000001	Plantae	Tracheophyta	Ginkgoopsida	Ginkgoales	Ginkgoaceae	Ginkgo	Ginkgo biloba	2126	981

DISTRIB_QDGC

taxonid	locid	first_occ	last_occ	no_date	n_occ	observation	literature	...	unknown
1000001	736540	1984	2011	FALSE	4	TRUE	FALSE	...	FALSE

DATA_QDGC

locid	longitude	latitude	elevation	elev_min	elev_max	elev_range	countryid	terr_ecoid	oceanid	mari_ecoid
736540	-4.875	37.875	248.707	77	581	504	724	181221	NULL	NULL

Elevation & Bathymetry data
Geopolitical & Ecological information

DATA_QDGC

bio1	...	bio19	ai	IceConc (*)	SST (*)	SSS (*)	diss_oxy	nitrate	phosphate	silicate
16.895	...	218.103	0.316	NULL	NULL	NULL	NULL	NULL	NULL	NULL

Figure 4. Structure of the gbif4crest PostgreSQL database. By default, the package extracts data from the TAXA, DISTRIB-QDGC and DATA-QDGC tables. The DISTRIB table contains the raw occurrence data obtained from GBIF and can be used to curate the distribution data at a different spatial resolution. Note that the DATA-QDGC table spreads across two rows on this figure.

the last observation dates. The `DATA_QDGC` table was also entirely recalculated using a new protocol that better accounts for coastal margins, implying that some coastal climate values may differ, however marginally, between the different versions of the *gbif4crest* dataset.

Due to its large size (about 15 Gb), this database is not downloaded when installing the package but can be accessed through different routes. First, the data are stored in an open-access, cloud-based PostgreSQL database that can be accessed via *crestr*. This solution is the recommended option, as users without any SQL knowledge can benefit from the package's interface to automatically query the database simply by providing study-specific parameters (*e.g.* the name of the taxa or geographical boundaries for the study area) to import all the necessary data in the correct format to the R environment (see Section 5.2). Second, more advanced users can also directly query the database to extract and curate data from the `DISTRIB` or `DISTRIB_QDGC` tables using SQL requests and the `dbRequest()` function. Finally, the full *gbif4crest* calibration dataset can also be downloaded as an SQLite3 portable database file from Chevalier (2020).

Table 1. List of terrestrial variables available for reconstruction in the *gbif4crest* database. Each one can be selected in *crestr* using its associated code. List of abbreviations: (Temp.) Temperature, (Precip.) Precipitation.

Terrestrial variables		
Code	Full name	Source
bio1	Mean Annual Temp. (°C)	Fick and Hijmans (2017)
bio2	Mean Diurnal Range (°C)	Fick and Hijmans (2017)
bio3	Isothermality (x100)	Fick and Hijmans (2017)
bio4	Temp. Seasonality (standard deviation x100) (°C)	Fick and Hijmans (2017)
bio5	Max Temp. of the Warmest Month (°C)	Fick and Hijmans (2017)
bio6	Min Temp. of the Coldest Month (°C)	Fick and Hijmans (2017)
bio7	Temp. Annual Range (°C)	Fick and Hijmans (2017)
bio8	Mean Temp. of the Wettest Quarter (°C)	Fick and Hijmans (2017)
bio9	Mean Temp. of the Driest Quarter (°C)	Fick and Hijmans (2017)
bio10	Mean Temp. of the Warmest Quarter (°C)	Fick and Hijmans (2017)
bio11	Mean Temp. of the Coldest Quarter (°C)	Fick and Hijmans (2017)
bio12	Annual precip. (mm)	Fick and Hijmans (2017)
bio13	Precip. of the Wettest Month (mm)	Fick and Hijmans (2017)
bio14	Precip. of the Driest Month (mm)	Fick and Hijmans (2017)
bio15	Precip. Seasonality (Coefficient of Variation) (mm)	Fick and Hijmans (2017)
bio16	Precip. of the Wettest Quarter (mm)	Fick and Hijmans (2017)
bio17	Precip. of the Driest Quarter (mm)	Fick and Hijmans (2017)
bio18	Precip. of the Warmest Quarter (mm)	Fick and Hijmans (2017)
bio19	Precip. of the Coldest Quarter (mm)	Fick and Hijmans (2017)
ai	Aridity Index (unitless)	Zomer et al. (2008)

4 The *crestr* R package

4.1 Philosophy of the package

The *crestr* package has been designed for two independent but complementary modelling purposes. The probabilistic proxy-climate responses can be used to quantitatively reconstruct climate from their statistical combination, such as in Chevalier et al. (2021a) or Chevalier and Chase (2015), or they can be used in a more qualitative way to determine the (relative) climate sensitivities of different taxa in a given area to characterise past ecological changes, such as in Chevalier et al. (2021b) or Quick et al. (2021). To simplify access to the functionalities, default values are provided for all parameters to enable a rapid generation of preliminary results that users can then use as a starting point to adapt the model to their data. Different publication-ready graphical diagnostic tools were designed to represent the CREST data in a standardised way to guide users in this task and avoid the typical ‘black box’ criticism many complex statistical tools face. These tools include plots of the calibration data, the

Table 2. List of marine variables available for reconstruction in the *gbif4crest* database. Each one can be selected in *crestr* using its associated code. List of abbreviations: (SST) Sea Surface Temperature, (SSS) Sea Surface Salinity.

Oceanic variables		
Code	Full name	Source
sst_ann	Mean Annual SST (°C)	Locarnini et al. (2018)
sst_jfm	Mean Winter SST (°C)	Locarnini et al. (2018)
sst_amj	Mean Spring SST (°C)	Locarnini et al. (2018)
sst_jas	Mean Summer SST (°C)	Locarnini et al. (2018)
sst_ond	Mean Fall SST (°C)	Locarnini et al. (2018)
sss_ann	Mean Annual SSS (PSU)	Zweng et al. (2018)
sss_jfm	Mean Winter SSS (PSU)	Zweng et al. (2018)
sss_amj	Mean Spring SSS (PSU)	Zweng et al. (2018)
sss_jas	Mean Summer SSS (PSU)	Zweng et al. (2018)
sss_ond	Mean Fall SSS (PSU)	Zweng et al. (2018)
icec_ann	Mean Annual Sea Ice Concentration (%)	Reynolds et al. (2007)
icec_jfm	Mean Winter Sea Ice Concentration (%)	Reynolds et al. (2007)
icec_amj	Mean Spring Sea Ice Concentration (%)	Reynolds et al. (2007)
icec_jas	Mean Summer Ice Concentration (%)	Reynolds et al. (2007)
icec_ond	Mean Fall Sea Ice Concentration (%)	Reynolds et al. (2007)
diss_oxy	Dissolved Oxygen Concentration (µmol/L)	Garcia et al. (2018a)
nitrate	Nitrate Concentration (µmol/L)	Garcia et al. (2018b)
phosphate	Phosphate Concentration (µmol/L)	Garcia et al. (2018b)
silicate	Silicate Concentration (µmol/L)	Garcia et al. (2018b)

estimated climate responses, the reconstructions and more. These figures allow looking at the data from different perspectives to help interpret the results and possibly identify potential issues or biases in the selected data and parameters. Such diagnostic tools are available for every stage of the process, and, as exemplified in Section 5, they can be generated with a single line of R code.

4.2 The central element: the `crestObj` object

In *crestr*, all the CREST-related data are stored within a single S3 object of the class `crestObj` that is first initialised by either `crest.get_modern_data` or `crest.set_modern_data` (see section 5.2 for details). Most package functions will take a `crestObj` as their primary input and return an updated version of that object. In practice, a `crestObj` is a nested list that contains five sub-lists, each one grouping a specific type of information, such as the calibration data, the fitted climate responses, or the reconstructions (Fig. 5). Wrapper functions have been implemented to manipulate and modify the information

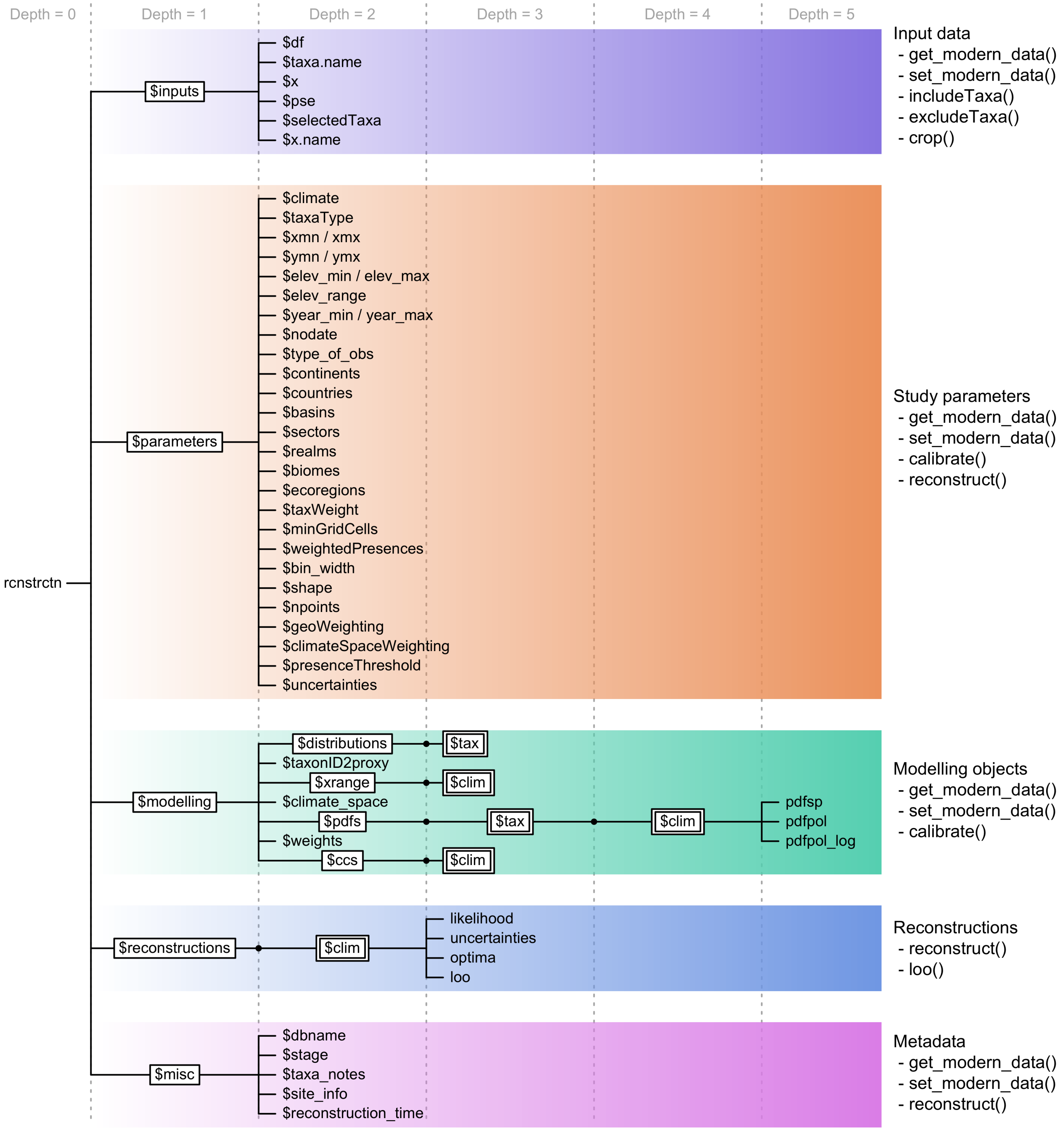

Figure 5. Structure of a crestObj, here called ’rcnstrctn’, with the five main sub-lists in colour. For simplicity, lists with many elements (’tax’ or ’clim’) are represented with double framed boxes. The unframed terminal nodes on the right-hand side of each branch are simple R objects, such as numbers, characters, vectors or data frames. The names of the functions that modify the objects in the sub-lists are indicated on the right.

contained in a `crestObj`, and users are never expected to manually modify their `crestObj`– even if it is possible. The five sub-lists contain the following information:

- `inputs`: contains the input data (*e.g.* the counts/percentages of the fossil proxy data, the ages of the samples or the names of the fossil taxa).
- `parameters`: contains the parameters provided at the different stages of the analysis (*e.g.* the tailoring of the *gbif4crest* calibration dataset or the fitting and combination of the PDFs; see Section 5).
- `modelling`: contains all the data related to the estimation of the PDFs (*e.g.* the occurrence data (the 'distributions') used to estimate the PDFs, the climate space of the study area, or the PDFs themselves).
- `reconstructions`: contains all the results (*e.g.* best estimates, synthetic error measurements, and the full distribution of the reconstruction).
- `misc`: contains some additional metadata relative to the reconstruction (*e.g.* the site location or, most importantly, information related to the proxy-species associated process described in section 4.3.2).

4.3 Input data for *crestr*

Five different input data files are compatible with *crestr*. However, most applications will only require two files (the `df` and `PSE` files, see below) to be created. More specific applications may require up to four of these files. All the files can be prepared outside the R environment and imported using standard R functions. Examples files based on pseudo data accompany the 'get started' example provided in the package (https://mchevalier2.github.io/crestr/articles/get-started.html). The files used in the application to illustrate the package are available as Supplementary Material to this paper.

4.3.1 The fossil data (`df`)

The `df` data frame is required if *crestr* is used for reconstructing climate and can be omitted if the objective is limited to modelling the climate response(s) of different taxa. `df` is a data frame with the samples entered as rows, with either the age, depth, or sample ID as the first column and the fossil data in the subsequent columns. `df` can contain raw counts, percentages, presence/absence data (1s and 0s) or even relative weights to be used in the reconstruction (see examples in Section 5.6).

4.3.2 The proxy-species equivalency (`PSE`) table

Creating a `PSE` data frame is required to extract distribution data from the *gbif4crest* calibration dataset. It is used to group individual species available in the `TAXA` table into their corresponding fossil taxon. This step is important to estimate the species responses ($\mathrm{PDF_{sp}}(s,c)$) and taxon responses ($\mathrm{PDF_{tx}}(t,c)$) described in Section 2.2. When all the fossil taxa are identified at the species level, the `PSE` table is a simple data frame with one row per taxon (such as, for instance, the row corresponding to *Elais guineensis* in Table 3). However, fossil taxa are most often identified at a lower taxonomic resolution (sub-genus, genus, sub-family, family). These varying levels of identification should be encoded in the PSE file to link one or more (groups of) species to their common fossil taxon name (*i.e.* group together all the species that are likely to have produced the observed fossil). Several species can be assigned to a taxon at once by limiting the taxonomic description at the family or genus level (*e.g. Artemisia* in Table 3).

Table 3. Example classification of four pollen taxa from the example case study, each one with a different level of taxonomic resolution. The last column 'Taxonomic resolution' is added here for explanatory purposes only and is not required in a real 'PSE' table.

Level	Family	Genus	Species	ProxyName	Taxonomic resolution
1	Asteraceae			Asteracae undiff.	Family
2	Asteraceae	*Stoebe*		*Stoebe*-type	Subfamily
2	Asteraceae	*Elytropappus*		*Stoebe*-type	Subfamily
2	Asteraceae	*Artemisia*		*Artemisia*	Genus level
3	Arecaceae	*Elaeis*	*Elaeis guineensis*	*Elaeis guineensis*	Species
4				Triletes spores	To be excluded

A PSE file is composed of five columns (Table 3). The first one (*Level*) contains an integer that indicates the level of taxonomic resolution of the row (1 for Family, 2 for Genus, 3 for Species and 4 for taxa that should be excluded from the reconstruction, *e.g.* 'Triletes spores' in the example case study). The fifth column, *ProxyName*, contains the name of the taxon. All the taxa recorded in the df dataset should be listed here, or they will be excluded from the study. Columns two to four contain the taxonomic classification of that taxon as *Family*, *Genus* and *Species*, respectively. For simplicity, a pre-formatted version of the PSE table with the names of all the taxa to study can be generated by *crestr* using the createPSE() function that generates a spreadsheet with the correct structure and with the *Level* and *ProxyName* columns automatically filled in:

```
list_of_taxa <- colnames(df)[-1]
createPSE(list_of_taxa)
```

The species-taxon association is performed in sequential steps by the crest.get_modern_data() function (see Section 5.2). First, *crestr* classifies the taxa with the lowest taxonomical resolution (*i.e.* when *Level* is equal to one) and then increases the resolution *Level* by *Level*. In the example in Table 3, different taxonomic resolution levels are provided for different plant species belonging to the highly diverse Asteraceae family (the daisy family). To distribute all the Asteraceae species observed across the study area to their appropriate taxon, all the species are first classified as 'Asteraceae undiff.' (first row, *Level* = 1). In subsequent steps, the classification of some of these Asteraceae species is refined when reaching the better-resolved sub-groups (*Stoebe*-type and *Artemisia* at *Level* = 2). At the end of the process, the 'Asteraceae undiff.' group only contains Asteraceae species that grow in the study area but are not part of the genera *Stoebe*, *Elytropappus* or *Artemisia*. The latter are categorised separately as *Stoebe*-type or *Artemisia*.

Additional taxa can also be added to the `PSE` file to exclude species known not to be part of a group, even if the pollen grains corresponding to these species have not been observed. For instance, this 'trick' could have been used to simplify the climate response of the 'Asteraceae undiff.' group by excluding more species from it. This categorisation process can be time-consuming, as all the taxa must be classified in a unique `PSE` table. This process will often require a few iterations to be optimised. The results of the different assignments are stored in the `crestObj` returned by the `crest.get_modern_data()` function and can be evaluated by checking `rcnstrctn$misc$taxa_notes`.

4.3.3 The alternative modern calibration dataset (`distributions`)

Users that prefer fitting proxy-climate responses from their own calibration data instead of the proposed *gbif4crest* dataset should prepare a `distributions` dataset following the specific structure presented in Table 4. The first two columns should contain species names (or any unique identifiers) and the corresponding proxy name. If more than one species correspond to one taxon, the PDFs will be fitted in two steps, as explained in section 2. The following two columns contain the coordinates of the species occurrence data. Finally, the last columns contain the climate values to be reconstructed. An optional column called `weight` can be added to `distributions` in the fifth position (*i.e.* between the coordinates and the climate variables) if one wants to weigh the different observations. For example, the (relative) abundance of taxa observed from modern proxy assemblages can be used when fitting the PDFs to give more importance to the observations where that abundance is highest. This could also be used if accurate abundance data were available instead of presence-only data. The weights take a value between 0 and 100.

Table 4. Template for the *distributions* data frame. The weights column, here indicated with a '*', is optional and can be omitted or its values all set to 1 to assign the same weight to each observation. The number of rows of the table should correspond to the number of unique occurrences available.

Species name	Taxon Name	Longitude	Latitude	Weight*	clim_1	...	clim_n
Stoebe plumosa	*Stoebe*-type	18.875	-34.375	20	15.8	...	711
Elytropappus rhinocerotis	*Stoebe*-type	18.375	-33.625	32	16.9	...	477
...	...	...	...	...	...	...	...
Elaeis guineensis	*Elaeis guineensis*	-4.375	10.875	4	27.4	...	1020

4.3.4 The `climate_space` data frame

This data frame is only necessary if the users use a personal calibration dataset (`distributions`) instead of the *gbif4crest* dataset. This data frame enables 1) using the climate space weighting option (Section 2.2) and 2) including plots of modern climate in the different diagnostic tools. Its structure is straightforward, with the first two columns containing longitudes and latitudes and the subsequent columns the climate variables to reconstruct. The spatial resolution and the ordering of the climate variables should be identical to the `distributions` table (Table 4). However, the arrangement of the rows is not important. Including a `climate_space` dataset is recommended, even if it is not mandatory.

4.3.5 The **`selectedTaxa`** data frame

The last data frame that may be used to inform the reconstruction is a data frame of ones and zeros called `selectedTaxa`. This data frame has as many rows and columns as there are taxa and climate variables, respectively. Each entry, which should be either 1 or 0, indicates if the taxon should be used to reconstruct the climate variable (value = 1) or not (value = 0). If a `selectedTaxa` data frame is not provided, a default data frame with all entries set to 1 is added to the `crestObj` at initialisation. Users can then modify this information at any point using the `includeTaxa()` and `excludeTaxa()` built-in functions. The `crest.get_modern_data()` function also modifies this data frame by setting the value to -1 when the `PSE` classification failed for a taxon or when the amount of data in the study area is insufficient to fit a reliable PDF (see the parameter description in section 5.2).

4.4 Package dependencies

The *crestr* package is built in R (R Core Team, 2020) using the `devtools` package (Wickham et al., 2020). *crestr* depends on numerous packages, including: `clipr` (Lincoln, 2020), `DBI` (R Special Interest Group on Databases (R-SIG-DB) et al., 2021), `openxlsx` (Schauberger and Walker, 2020), `pals` (Wright, 2021), `plot3D` (Soetaert, 2021), `plyr` (Wickham, 2011), `raster` (Hijmans, 2021), `rgdal` (Bivand et al., 2021), `rgeos` (Bivand and Rundel, 2020), `RPostgres` (Wickham et al., 2021), `scales` (Wickham and Seidel, 2020), `sp` (Pebesma and Bivand, 2005, Bivand et al. (2013)), `stringr` (Wickham, 2019) and `viridis` (Garnier et al., 2021). The dedicated documentation, tutorials and application examples found at https://mchevalier2.github.io/crestr were generated and formatted by the package `pkgdown` (Wickham and Hesselberth, 2020).

5 Step-by-step user guide for *crestr*

5.1 Example application: Pollen-based Mean Annual Temperature reconstructions from marine core MD96-2048

To illustrate the different ways of using *crestr* and its graphical diagnostic tools, I use pollen data recently analysed with the original CREST software to reconstruct mean annual temperature (MAT) from marine core MD96-2048. The core was retrieved off the coast of South Africa and Mozambique near the mouth of the Limpopo River. The terrestrial sediments are expected to come from the entire catchment of the Limpopo River and the smaller local river catchments near the coast (Dupont et al. (2019), Dupont et al. (2011), Castañeda et al. (2016)). The MAT reconstruction is based on 181 fossil pollen samples and the percentages of more than 150 terrestrial pollen taxa and covers the last 790,000 years.

As the catchment of these marine sediments is large, an extensive calibration dataset covering all vegetation zones from tropical Africa to the temperate southwestern tip of South Africa was designed to prevent any artificial reduction in the possible range of variability of the reconstruction. The glacial-interglacial trends and amplitude of the MAT reconstructions were validated by comparing them with regional temperature records and other global indicators of glacial-interglacial temperature variability (*e.g.* Antarctic temperature or global sea-level curves, see Chevalier et al. (2021a) for more details). Here, I reproduce this reconstruction using the original parameterisation of the CREST algorithm obtained from the original CREST point-and-click interface to showcase how it can easily be replicated in a few lines of code with the *crestr* package. Due to the update of the climate data of the calibration dataset described in section 3, marginal differences in the order of tenths of Celsius degrees can, however, be observed between the original publication and this reproduction. All the necessary datasets and R code are available as supplementary material.

5.2 Formatting the calibration data in a `crestObj`

As the *gbif4crest* dataset was used to fit the PDFs, the function called `crest.get_modern_data()` was used to extract the calibration data:

```
rcnstrctn <- crest.get_modern_data(
  df = MD96_2048,
  pse = PSE,
  selectedTaxa = selectedTaxa,
  taxaType = 1,
  climate = c('bio1'),
  xmn = NA, xmx = NA,
  ymn = -35, ymx = NA,
  continents = 'Africa',
  countries = c('South Africa', 'Kenya',
    'Lesotho', 'eSwatini', 'Botswana',
    'Mozambique', 'Zimbabwe', 'Zambia',
    'Malawi', 'Tanzania', 'Namibia',
    'Uganda', 'Rwanda', 'Burundi'),
  realms = NA,
  biomes = NA,
  ecoregions = NA,
  minGridCells = 20,
  site_info = c(34.0167, -26.1667),
  site_name = 'MD96-2048',
  dbname = "gbif4crest_02",
  verbose = TRUE
)
```

All the parameters of the function were defined by the characteristics of the proxy (pollen), the climate to reconstruct (MAT / bio1) and the definition of the study area (East and southern Africa). The three input files (*i.e.* `df`, `PSE` and `selectedTaxa`; see section 4.3) required to realise this reconstruction are reproduced from the published dataset (Chevalier et al., 2020a) and are available in Supplementary Material. The following points describe the different parameters of the `crest.get_modern_data()` function and how they relate to the data extraction and modelling.

- The parameter `taxaType` is used to choose the type of proxy used and takes a value between 1 to 6 for plants (*i.e.* pollen and plant macro remains), beetles, chironomids, foraminifers, diatoms and rodents, respectively.

- The name(s) or code(s) of the `climate` variables to study should be provided here (see Tables 1 and 2 or use the function `accClimateVariables()` for a list of accepted names). Here, ‘bio1’ means mean annual temperature. More variables can be added if necessary (*e.g.* `c('bio1', 'ai')`). However, serial reconstructions should be avoided, even if many variables are provided with this package. Careful interpretations of the fossil data should be made before selecting variables.

- Geographical parameters can be provided to tailor the *gbif4crest* dataset to the study area and data. These can include minimum and maximum longitude and latitude (`xmn`, `xmx`, `ymn`, `ymx`), continent, ocean or country names (see `accCountryNames()` and `accBasinNames()` for a list of accepted names), and also some ecological classifiers, such as realms, biomes or ecoregions (see `accRealmNames()` for a list of official names). Only the occurrences that respect all the specified constraints will be returned.

- To estimate reliable species PDFs, it is recommended to use at least 20 distinct occurrences for each species, even if different values can be specified with the `minGridCell` parameter, depending on the density of data available across the study area.

- Optional information about the site, such as a name and coordinates, can be provided and, where possible, this information will be represented on the different graphical diagnostic tools created by *crestr* (*e.g.* the location of the record is added to the maps if the coordinates are provided).

The `crest.get_modern_data()` function reads all the data and parameters, extracts the data from the cloud-based *gbif4crest* database, processes the distribution data and returns everything as a structured `crestObj` – here called `rcnstrctn` and whose structure is displayed on Fig. 5 – that will be read and modified by all subsequent functions. Alternatively, the function `crest.set_modern_data()` could be called instead of `crest.get_modern_data()` to use personal calibration data instead of the *gbif4crest* database. If the calibration data needed for this study were available as a `distributions` and `climate_space` data frames (Section 4.3), similar results would be obtained with:

```
rcnstrctn <- crest.set_modern_data(
  df = MD96_2048,
  distributions = distributions,
  climate_space = climate_space,
  selectedTaxa = selectedTaxa,
  climate = c('bio1'),
  weight = FALSE,
  minGridCells = 20,
  site_info = c(34.0167, -26.1667),
  site_name = 'MD96-2048',
  verbose = TRUE
)
```

5.3 Estimating the climate responses (the PDFs)

The probabilistic proxy-climate responses, *i.e.* the PDFs, are estimated from the presence-only data using the `crest.calibrate()` function:

```
rcnstrctn <- crest.calibrate(
  rcnstrctn,
  shape = c('normal'),
  climateSpaceWeighting = TRUE,
  bin_width = c(2),
  npoints = 500,
  geoWeighting = TRUE,
  verbose = TRUE
)
```

As described in Section 2.2, the different parameters that control the reconstruction should be carefully considered to produce reliable PDFs. These include specifying:

- the `shape` of the species PDFs, which should be either 'normal' or 'lognormal', depending on the variable to reconstruct (see Section 2.2).
- the width of the climate bins (`bin_width`) expressed in the variables' units (*e.g.* 2°C or 50 mm) if the PDFs are corrected for an heterogeneous climate space (`climateSpaceWeighting` set to `TRUE`). Dividing the total climate space in 15-25 bins often leads to good results, but other values are possible.
- the number of intervals required to divide the studied climate range and fit the PDFs `npoints`. This will ultimately define the climate resolution of the reconstructions. *crestr* runs faster with lower values, but this can alter the reconstructions with visible 'jumps' between consecutive climate values (aliasing effect).

  - set `geoWeighting` to `TRUE` if the species PDFs of the different composing species should be weighted according to the square-root of the extent of their modern distribution (the $\sqrt{\mathrm{N}_s}$ in Eqt. 6).

5.4 Assessing the coherency of the climate space

In every study involving estimating relationships between biological entities and environmental parameters, the first step is to ensure that the defined study area and associated calibration dataset are coherent. This includes ensuring that 1) all the essential taxa observed in the past are present in the study area, and their distributions are not truncated, 2) the climate values to reconstruct are likely to be covered by present-day climate values (the reconstructions are bounded by the lowest and highest values observed in the modern climate space) and 3) there is no large sampling or representativity bias (*e.g.* along country borders due to different sampling efforts). The 'climateSpace' graphical diagnostic tool (Fig. 6) was designed for a rapid assessment of all these characteristics:

```
plot_climateSpace(rcnstrctn, save=TRUE,
  filename='Figure 6.png',
  as.png=TRUE, png.res=600,
  width=6.9, height=4.4,
  y0=0.4,
  add_modern=TRUE
)
```

Ideally, the climate values sampled by the calibration data should be as homogeneous as possible to ensure proper representation of all the possible climate values, even if the extreme climate values will always be under-represented compared to the median ones. However, deviations from a theoretical equivalence between the observed climate distribution and the climate values sampled by the calibration data are not necessarily a bad characteristic. In our case study, the variability of the sampling density represents actual patterns in regional species diversity with the presence of several biodiversity hotspots across the mountainous regions of eastern and southern Africa (Myers et al., 2000). This higher diversity in the colder areas explains why the black histogram (*i.e.* the climate values associated with occurrence data) on Fig. 6 is skewed towards the left compared to the grey histogram (*i.e.* the distribution of the climate space in the study area). All these elements should be checked and accounted for while designing the final calibration dataset.

The 'climateSpace' diagnostic figure is also practical for identifying potential local or global correlations between different climate variables and assessing the risk of confounding variables (*i.e.* variables that are correlated with important variables but do not directly impact the studied proxies; Juggins (2013), Chevalier et al. (2020b)). Any change to the parameters related to the definition of the climate space (*e.g.* definition of the study area, climate variables to reconstruct) will require re-running `crest.get_modern_data()` or `crest.set_modern_data()` with updated parameters and/or data.

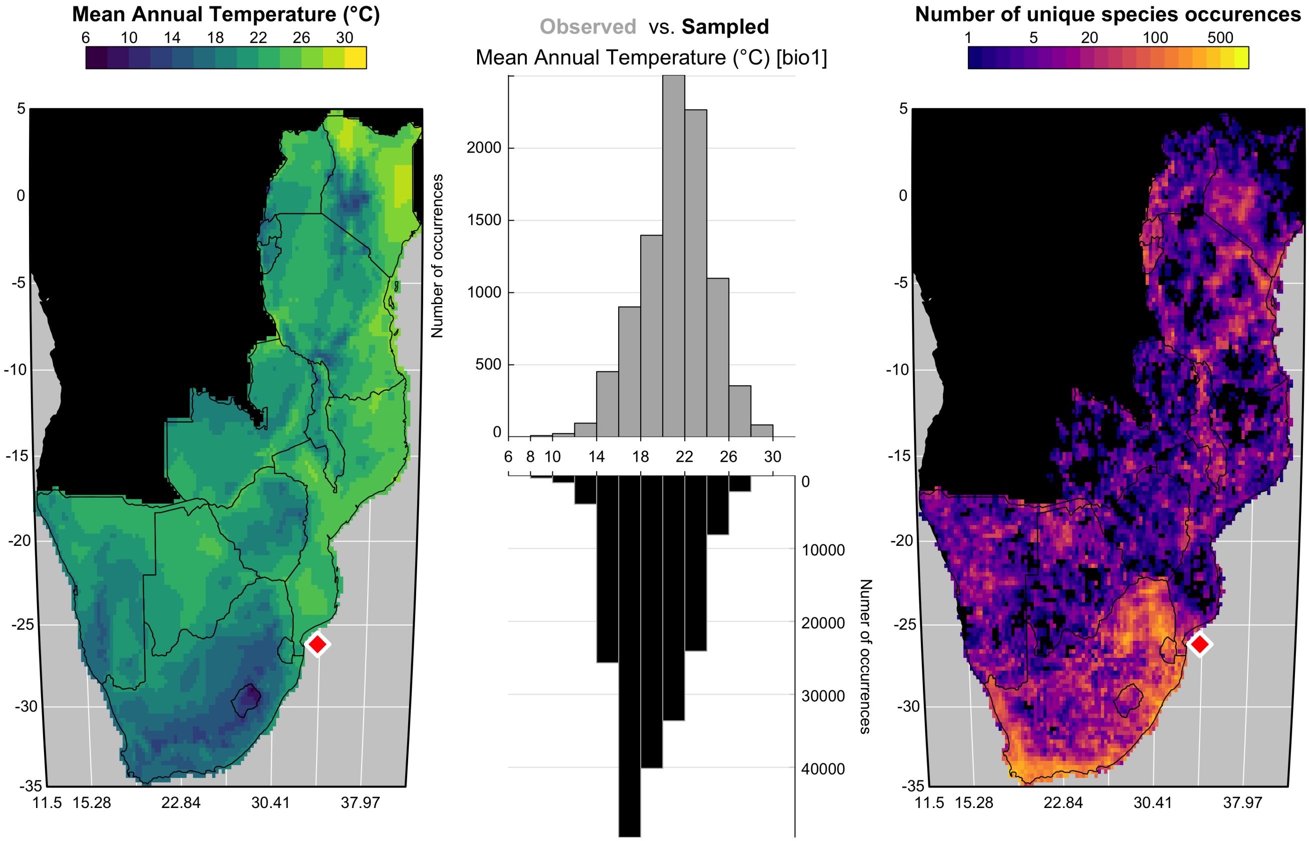

Figure 6. 'climateSpace' graphical diagnostic tool to evaluate the calibration dataset. The map on the right represents the density of unique species occurrences in each grid cell, highlighting a certain bias towards South Africa. The lower abundance of plant data available from Angola and the Democratic Republic of Congo (data not shown) is the reason why these two countries were excluded from the study area. The map on the left represents the studied climate variable (MAT) across the study area. The double histogram in the middle represents the distribution of MAT (the climate space in grey, top), while the black histogram (bottom) represents how the calibration data sample the climate space. Differences between the two histograms can be used to identify biases in the calibration dataset. Here, the small shift of the black histograms towards colder values (towards the left) is another way of seeing that more data are available from South Africa than other countries and reflects, in part, the regional patterns of biodiversity. If more variables had been selected in this study, additional rows would be added to the figure with a similar climate map and histograms and a scatterplot of the climate variables to highlight potential local or regional modern correlations.

5.5 Assessing the coherency of the climate responses

With the study area and climate space defined, the next step is to search for taxa that show specific relationships with climate. While all species eventually respond to all climate variables, they can be more sensitive to one over another within a given region. The low taxonomic resolution of some fossil proxies, such as pollen data, can also mask strong species-climate relationships (Chevalier et al., 2021b). Looking at each individual climate response(s) and assessing their significance within the boundary conditions of the study is thus critical. The ‘taxaCharacteristics’ diagnostic plot (Fig. 7) was designed for this task:

```
plot_taxaCharacteristics(rcnstrctn,
  taxanames='Ericaceae', save = TRUE,
  filename = 'Figure 7.png',
  as.png=TRUE, png.res=600,
  width=6.9, height=8.13,
  add_modern=TRUE
)
```

One summary plot can be generated for every taxon to assess and inter-compare their geographical distributions and climate responses. As illustrated in Fig. 7, Ericaceae is preferentially observed in the colder environments of the study area, its higher percentages occur during glacial periods, and a coherent response of all its composing species can be observed despite a high diversity (141 species with at least 20 unique occurrences across the study area). All these elements indicate that Ericaceae can be considered a cold environment indicator in eastern and southern Africa. Sensitivities to other variables can also be expected but are not considered in this study. Similar sensitivity inferences can be made to define a list of temperature-sensitive taxa to reconstruct MAT (Chevalier and Chase (2015), Chevalier et al. (2021a)) or support qualitative interpretations of palaeoecological datasets (Chevalier et al. (2021b), Quick et al. (2021)). A complementary diagnostic plot to assess climate sensitivities is the ‘violinPDFs’ (Fig. 8):

```
tax <- sample(rcnstrctn$input$taxa.name,
              15, replace=FALSE)

plot_violinPDFs(rcnstrctn,
  taxanames = tax,
  save = TRUE,
  filename = 'Figure 8.png',
  as.png=TRUE, png.res=600,
  width = 6.9, height = 3,
  ylim=c(0,30)
)
```

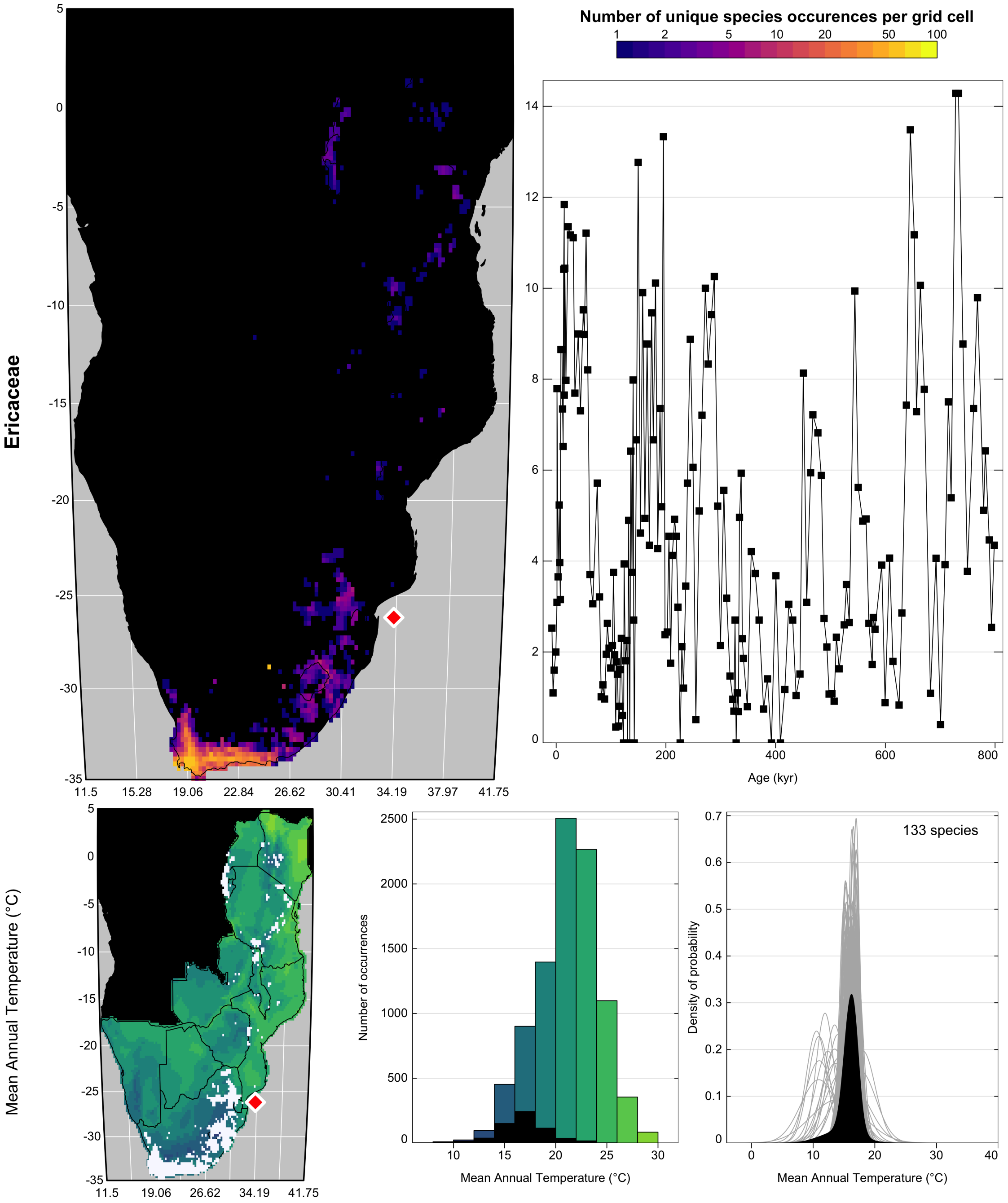

Figure 7. 'taxaCharacteristics' graphical diagnostic tool to assess the sensitivity of taxa to climate. In the top row, the map represents the density of unique species occurrences per grid cell derived from the modern calibration dataset, and the time series represents the variability of the taxon against time or depth. The bottom row is specific to each selected variable (only one row in this case). The map represents the geographical distribution of the taxon (in white) against the climate background. The histogram represents the climate space (in colour) and how this climate is sampled by the taxon (in black). Finally, the right plot represents the climate response of the taxon (in black) and the response of all the composing species (in grey). Overall, this figure highlights that despite its high diversity, Ericaceae is primarily associated with the colder environments of the study area and its presence increases during glacial periods. The red diamond indicates the location of the studied record.

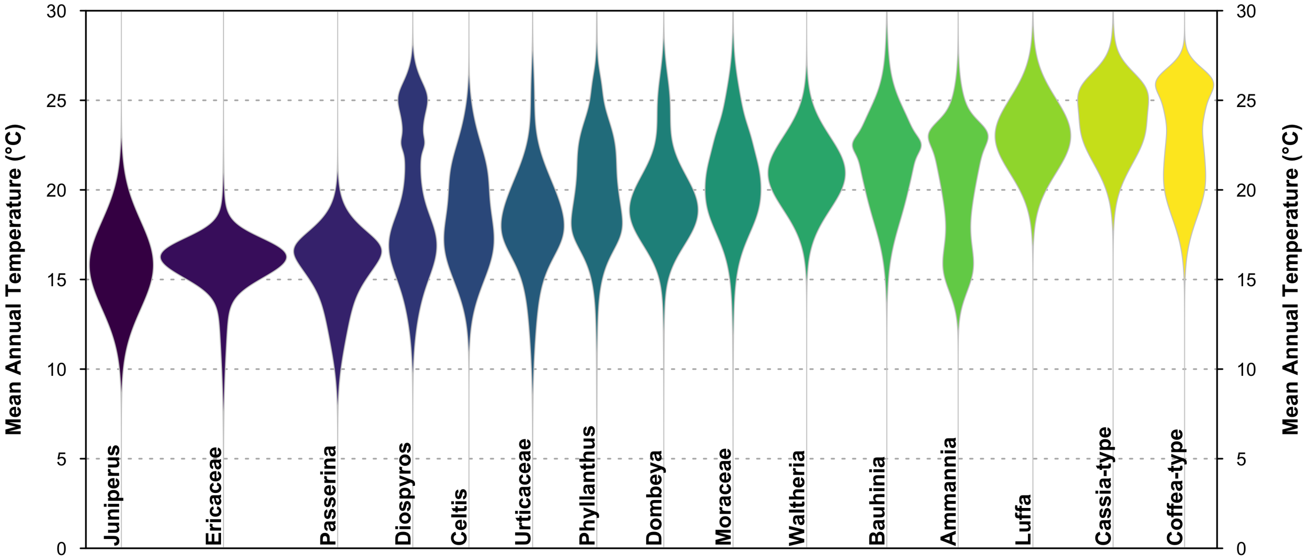

Figure 8. 'violinPDFs' graphical diagnostic tool to represent the PDFs of various taxa (here a random selection of 15 taxa). The taxa are sorted and colour-coded by their temperature optima (i.e. the temperature corresponding to the peak of their PDFs).

The violin plot represents the PDFs of a selection of taxa on the same plot, which helps compare the shape and spread of the different responses. All the violins have the same area (all the probabilities sum to 1), and the taxa are ranked by increasing values of their temperature optima (*i.e.* the temperature corresponding to the peak of the PDF). However, due to the possible multimodality of the PDFs and differences in tolerance ranges, this ranking does not mean that a taxon on the left always represents colder conditions than a taxon on the right. This is illustrated in many ways on Fig. 8 with, for example, *Cassia*-type that is estimated to experience warmer conditions than *Coffea*-type ~61% of the time (based on 100,000 random draws from their PDFs) despite having a 'colder' climate optimum, or with *Diospyros* that can tolerate much warmer conditions than most taxa with warmer optima. This type of representation can be beneficial to make more informed interpretations of ecological changes from pollen diagrams (Chevalier et al., 2021b, Quick et al. (2021)).

5.6 Reconstructing climate

Along with the `df` data frame provided to the `crest.get_modern_data()` or `crest.set_modern_data()` functions, a set of reconstruction parameters have to be chosen to combine PDFs and estimate climate parameters. The `selectedTaxa` data frame stored in the `crestObj` (see Fig. 5) defines the taxa that will be used to reconstruct each climate variable (by default, all taxa are included if sufficient data are available to fit a PDF). This selection can be modified by using the `includeTaxa()` and `excludeTaxa()` functions. For instance, both Aizoaceae and Chenopodiaceae/Amaranthaceae were excluded from the reconstruction because these taxa are not primarily sensitive to temperature in southern Africa. This can be simply done as follow:

```
rcnstrctn <- excludeTaxa(rcnstrctn,
  taxa=c('Aizoaceae',
     'Chenopodiaceae/Amaranthaceae'),
  climate=c('bio1')
)
```

Climate reconstructions are then performed with the `crest.reconstruct()` function:

```
rcnstrctn <- crest.reconstruct(
  rcnstrctn,
  presenceThreshold = 0,
  taxWeight = "normalisation",
  verbose = TRUE
)
```

A minimum 'presence threshold' below which the taxa will always be considered absent can be provided to reduce the noise of the fossil dataset (*e.g.* pollen percentages lower than 1 or 2% are commonly excluded from reconstructions, Chevalier et al. (2020b)). When `presenceThreshold` is set to zero, as is the case here, all the strictly positive pollen percentages are considered as actual presences and used accordingly to reconstruct MAT. To weigh the taxa as described in Eq. 7, four options are available in *crestr*:

- The data can be converted to presence/absence with all the values above and below `presenceThreshold` being changed to ones and zeros, respectively. This option is recommended for data such as macrofossils for which relative abundances cannot be reliably estimated.
- The data can be converted to percentages to weigh the taxa according to their relative abundance. This option is recommended for data where reliable proportions can be estimated.
- The data can be normalised following the method proposed by Chevalier et al. (2014) and described here by Eq. 8. This option is recommended for palaeoecological proxies where the observed percentages are not proportional to their abundance in the environment, such as pollen data.
- The data can be directly weighted by the values provided in `df`, which implies that users can define their own specific weighting strategy (e.g. using the square-root transformation of the pollen percentages).

5.7 Analysing and understanding the reconstruction(s)

Characterising the dominant factors that define a reconstruction can be difficult. This section presents three different graphical diagnostic tools that provide different perspectives on the reconstructed data and help look inside the statistical black box.

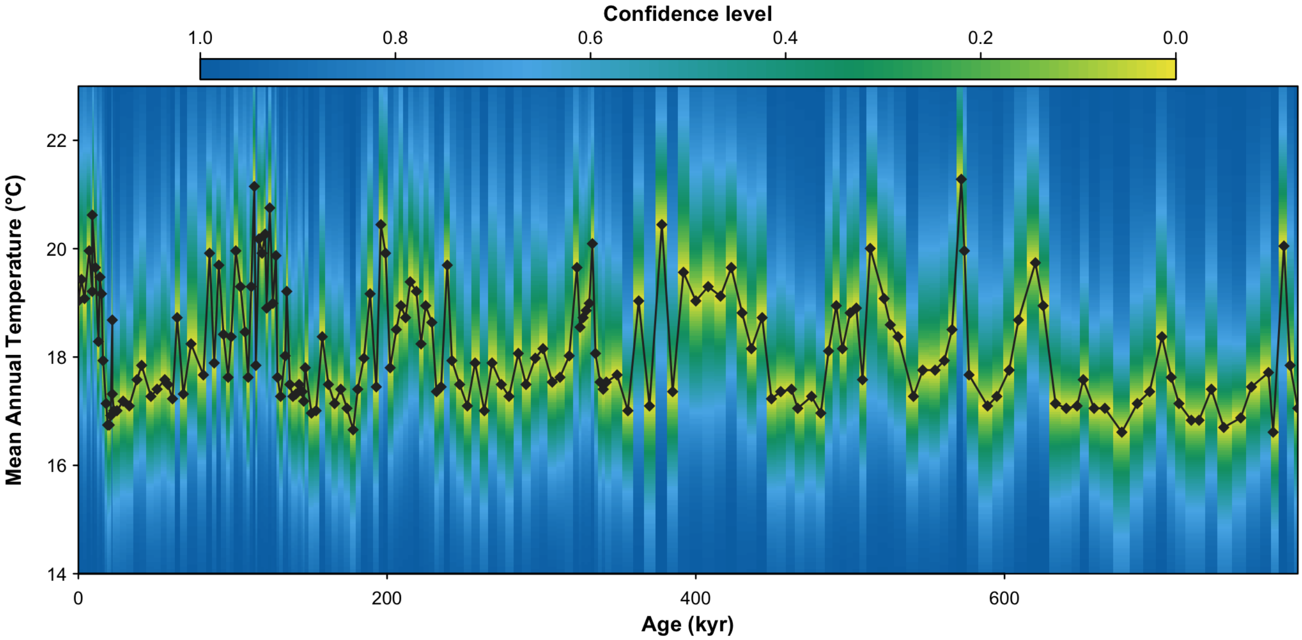

Figure 9. MAT probabilistic reconstructions for marine core MD96-2048. The yellow-green-blue colour gradient represents the uncertainties associated with each sample. This reconstruction is identical to the reconstruction presented in Chevalier et al. (2021) and the reader is referred to this publication for an in-depth validation and discussion of these results.

First, the full probabilistic breadth of the reconstructions can be represented by using the standard R `plot()` function (Fig. 9), which has been adapted to plot data stored in a `crestObj`:

```
plot(rcnstrctn,
  filename=’Figure 9.png’,
  save=TRUE,
  as.png=TRUE, png.res=600,
  width=6.9, height=3.54,
  ylim=c(14,23), uncertainties=1,
  simplify=FALSE,
  col=plot3D::gg2.col(200)[1:100],
  pt.cex=0.8, pt.lwd=1, pt.col=’#2c2c2c’
)
```

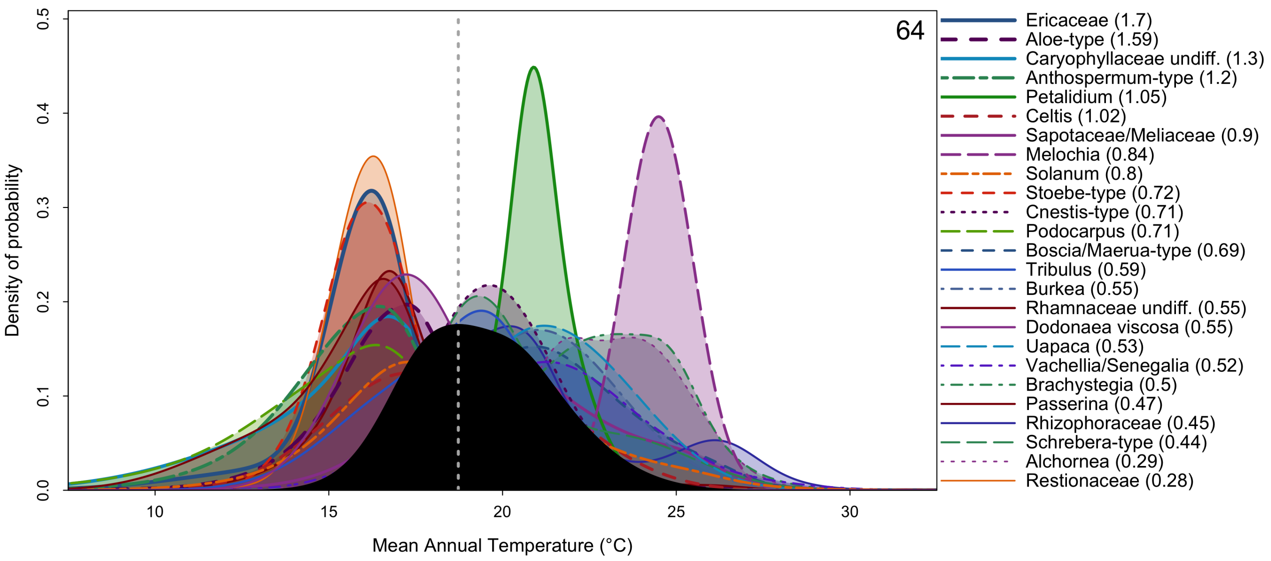

Figure 10. 'combinedPDFs' graphical diagnostic tool that shows the combination of the PDFs (in colour) of all the taxa recorded in the sample dated at 64 kyr. The thickness of the lines is related to the weight of the taxa in the sample (absolute value indicated next to each taxon name). The black curve represents the MAT reconstruction, from which a 'best' climate estimate can be estimated from the maximum of the curve (grey dashed line) and uncertainties derived by calculating the area under the curve.

While the probabilistic representation of the data should be preferred because it represents all the information available, a simpler version of this plot with the climate optima and more common uncertainty ranges expressed as colour bands can be obtained by specifying `simplify=TRUE` (not shown).

The `plot_combinedPDFs()` function can then be used to identify the taxa that are driving the reconstruction by focusing on the sample level:

```
plot_combinedPDFs(rcnstrctn,
    samples=3, only.present=TRUE,
    only.selected=TRUE, save = TRUE,
    filename = 'Figure 10.png',
    as.png=TRUE, png.res=600,
    width=6.9, height=3,
    xlim=c(7.5,32.5)
)
```

In this plot (Fig. 10), the PDFs of all the taxa present in the sample and selected to reconstruct the climate variable are represented along with the reconstruction. This type of plot can help identify if a particular PDF is at odds with the general assemblage, which usually indicates the possible presence of a confounding factor. It is also helpful to visualise the full spread of the uncertainties and, by extension, highlight that reconstructions can be multimodal. While it is not the case in the example here, multimodality can be the underlying cause of apparent noise in the reconstructions with minor changes in the taxa composition or percentages forcing the system to oscillate between two maxima and thus ‘appear’ noisy. This effect could also be seen from the reconstruction plot where the full uncertainties would be represented (`simplify=FALSE`).

Finally, a standard post-processing analysis of CREST reconstructions is a form of leave-one-out (LOO) analysis that is done with the `loo()` function:

```
rcnstrctn <- loo(rcnstrctn,
  verbose = TRUE
)
```

In the CREST context, a LOO analysis consists of repeatedly ‘unselecting’ one taxon at a time, running the reconstruction without that taxon and measuring the associated reconstruction anomalies. In our example, a positive anomaly means that the reconstruction without the taxon is warmer and, by extension, that the taxon is a cold indicator relative to a specific assemblage. A detailed analysis of the results can contribute to a deeper understanding of which taxa are the most important in driving the reconstructed climate signal. Taxa that exhibit large LOO values indicate a strong influence on the reconstruction. However, it does not necessarily mean that they are strong climate indicators. Large LOO values can arise when the PDFs are biased by unaccounted factors and are, as a result, at odds with the rest of the PDFs. Such factors can, for instance, include an incomplete estimate of the climate responses, which induces a bias or shift of the climate preferences, or a sensitivity of the taxon to other climatic (*e.g.* aridity instead of temperature) or non-climatic (*e.g.* edaphic conditions) factors. It is usually preferable to exclude such taxa from the reconstruction (*e.g.* Chenopodiaceae and Aizoaceae in our example).

The LOO analysis is a powerful tool to understand the taxa that primarily drive the reconstruction, and the LOO results can be represented as a typical stratigraphic diagram, where each row illustrates the effect of removing a taxon from the reconstruction (Fig. 11):

```
tax <- rcnstrctn$inputs$taxa.name[6:25]
plot_loo(rcnstrctn,
    taxanames=tax,
    xlim=c(0, 340), save = TRUE,
    filename = ’Figure 11.png’,
    as.png=TRUE, png.res=600,
    width=3.5, height=8,
    bar_width=3, col_neg=’coral3’,
    col_pos=’darkcyan’
)
```

For example, the expected cold effect of including Ericaceae on the MAT reconstructions from the MD96-2048 pollen record is immediately visible on Fig. 11. Similarly, the effect of removing either Ericaceae or Caryophyllaceae undiff. from the sample dated at 64 kyr (represented on Fig. 10) is quite strong with a warming of the reconstruction of 1.19 and 0.44°C, respectively. This type of plot can thus be used for both global and sample-specific inferences about the drivers of the reconstruction. Depending on the vegetation composition, some taxa can even sometimes be categorised as cold indicators when the assemblage represents warm conditions or warm indicators when the assemblage represents cold conditions (*e.g. Hypoestes/Dicliptera*-type on Fig. 11).

5.8 A wrapper function

To simplify the use of the package, the three stages of the reconstruction process – data acquisition (`crest.get_modern_data()` or `crest.set_modern_data()` if the *gbif4crest* dataset is not used), calibration (`crest.calibrate()`) and reconstruction (`crest.reconstruct()`) – can be called in one line of code using the wrapper function `crest()`. This function takes the same parameters described in this ‘step-by-step’ guide with the same default values and may be more practical when reconstructing several records in one run.

5.9 Exporting the reconstructions

All the data stored in the `crestObj` can be easily exported from the R environment as spreadsheets and RData files using either `export_pdfs()` to save the climate responses of the studied taxa or `export()` to save the reconstructions and many associated data in a publishable format. The latter also saves the `crestObj` as an RData file for easy reloading and sharing of the data:

```
export(rcnstrctn,
  loc='path/to/folder',
  fullUncertainties = TRUE,
  loo = TRUE,
  weights = TRUE,
  pdfs = TRUE
)
```

5.10 Citing building elements

Finally, all the reconstructions derived from *crestr* are built on numerous independent research efforts, including data compilations, modelling projects, statistical developments and software engineering. To support the long-term growth and visibility of all these building elements, it is crucial always to acknowledge them, even if their processing is invisible to the users. The list of references that must be cited for each use of *crestr* is automatically included in the summary tab of the spreadsheet generated by the `export()` function. In addition, the citation information can also be directly obtained from R using:

```
cite_crest(rcnstrctn)
```

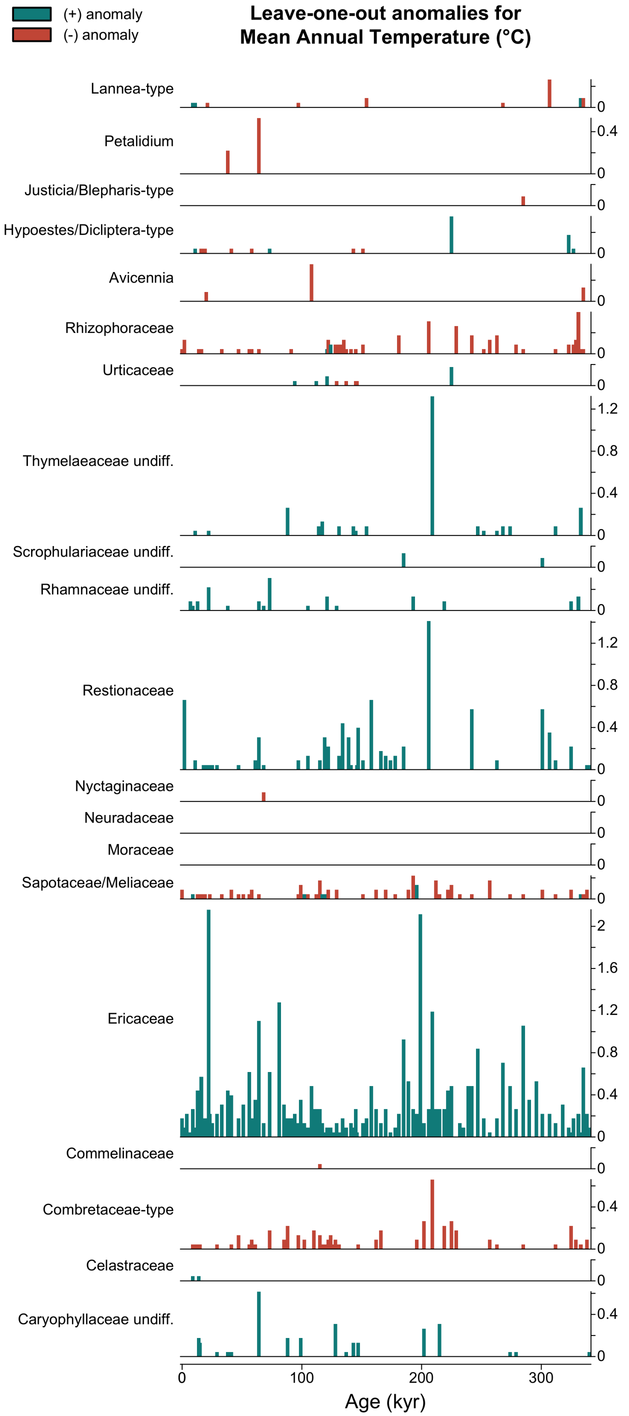

Figure 11. Leave-one-out (LOO) graphical diagnostic tool to illustrate the influence of different taxa on the reconstructions. Here, the results are only shown for a subset of the taxa observed in marine core MD96-2048 (only 20 out of the 171 available taxa are represented). The height of each bar represents the absolute effect (in °C) of removing the taxon from the reconstruction, and the sign of this effect (increase or decrease of the reconstructed temperature) is colour-coded. Here, blue (cf. Ericaceae) and red (cf. Combretaceae-type) bars indicate that the taxon is a cold and warm indicator, respectively, in the sample.

The function looks at the type of data used in the analysis (*e.g.* the subset of the GBIF data were used and the climate variables) and returns a corresponding list of references. For example, a simple way of crediting all the contributors for the MAT reconstruction from marine core MD96-2048 presented here could be the following: *"To create this MAT reconstruction from the pollen record from marine core MD96-2048 (Dupont et al. (2019)), we employed the CREST method (Chevalier et al. (2014), Chevalier (2019)). The PDFs were estimated by combining the MAT field of Fick and Hijmans (2017) and plant occurrence data from GBIF (GBIF (2020m), GBIF (2020k), GBIF (2020g)). The numerical analyses were realised with the crestr R package v1.0.1 (this reference)."*

6 Perspectives and conclusion

CREST is a probabilistic framework designed to model proxy-climate relationships from modern presence observations and to use these relationships to reconstruct past climate (Chevalier et al., 2014). The method's mathematics and assumptions enable an easy application everywhere, even in data-sparse regions. While developments to complexify the method are possible, the current version of the algorithm has proven to be reliable at producing high-quality reconstructions. The first version of the *crestr* R package is thus dedicated to implementing the original version of the algorithm. It also replaces the original point-and-click CREST software, which was challenging to maintain over time. A critical novelty of *crestr* is the inclusion of the CREST algorithm in a programmatic environment. The benefits of this transition are significant and include improved scriptability (*i.e.* the possibility of analysing many records automatically and sequentially), reproducibility (*i.e.* the capacity to reproduce an analysis) and better inter-operability (*i.e.* R packages are compatible with all computer systems). However, maintaining the highest level of accessibility remained at the core of the development process and is illustrated in the final product by the small number of functions necessary to run a complete analysis and the suite of detailed graphical diagnostic figures. In line with the objectives of the original software, the *crestr* package is aimed at all researchers interested in using CREST to reconstruct climate from palaeoecological datasets, including those with limited coding expertise.

In addition, its broad applicability will allow taking advantage of the recent growth of curated, open-access fossil datasets that offer unprecedented opportunities to reconstruct climate from a wide range of proxies, particularly in regions where quantified climate reconstructions are urgently needed. This package will thus also contribute to the current transition from single-site to multi-site studies, which is necessary to better understand past climate dynamics. However, it is essential to remember that running such techniques on several datasets should always be done carefully, as many factors can impact the reconstruction process. In practice, calibration datasets, variable selection and reconstructions should be assessed, ideally against independent evidence when they are available, even if there is no single way to validate a reconstruction (but see Chevalier et al. (2020b) for some discussions on the generic principles).

Over time, the *crestr* package will be enriched with new functionalities to facilitate reconstruction validation. The online documentation will also be updated with diverse examples and tutorials based on real applications and assessments (https://mchevalier2.github.io/crestr/). Future package updates will include Bayesian modules and propose more complex strategies to estimate proxy-climate relationships from data-dense regions. Finally, bug reports, feedback, and suggestions for newer functionalities and graphical diagnostic tools are encouraged and can be transmitted to the author directly or through GitHub's bug report portal (https://github.com/mchevalier2/crestr/issues).

Code and data availability. The *crestr* package is currently accessible from CRAN (https://cran.r-project.org/package=crestr). It is also available on GitHub (https://github.com/mchevalier2/crestr), where I also welcome feedback and strongly encourage contributions via the issue tracker (https://github.com/mchevalier2/crestr/issues). The source data used for the example application (pollen record from marine core MD96-2048 and associated temperature reconstructions) can be accessed from https://doi.pangaea.de/10.1594/PANGAEA.915923.

Competing interests. The author declares no competing interests.

Acknowledgements. This research has been supported by the Swiss National Science Foundation (grant no. CRSK-2_195875), with additional support from the University of Lausanne. MC is also supported by the German Federal Ministry of Education and Research (BMBF) as a Research for Sustainability initiative (FONA; https://www.fona.de/en, last access: 15 December 2021) through the PalMod Phase II project (grant no. FKZ: 01LP1926D). I thank Brian Chase, Yoshi Maezumi, Lynne Quick, Kale Sniderman and, last but not least, Mine Altinli for their invaluable feedback on early versions of the package and manuscript. NOAA High-Resolution SST data were provided by the NOAA/OAR/ESRL PSL, Boulder, Colorado, USA, from their Web site at https://psl.noaa.gov/data/gridded/data.noaa.oisst.v2.highres.html. And finally, I would also like to address a special thanks to the rticles contributors for their Climate of the Past Rmarkdown template!

References

Amante, C. and Eakins, B. W.: Etopo1 1 Arc-Minute Global Relief Model: Procedures, Data Sources and Analysis, NOAA Technical Memorandum NESDIS NGDC-24. National Geophysical Data Center, NOAA, https://doi.org/10.7289/V5C8276M, 2009.

Birks, H. J. B., Heiri, O., Seppä, H., and Bjune, A. E.: Strengths and weaknesses of quantitative climate reconstructions based on Late-Quaternary biological proxies, The Open Ecology Journal, 3, 68–110, https://doi.org/10.2174/1874213001003020068, 2010.

Bivand, R. and Rundel, C.: rgeos: Interface to Geometry Engine - Open Source ('GEOS'), https://CRAN.R-project.org/package=rgeos, r package version 0.5-5, 2020.

Bivand, R., Keitt, T., and Rowlingson, B.: rgdal: Bindings for the 'Geospatial' Data Abstraction Library, https://CRAN.R-project.org/package=rgdal, r package version 1.5-23, 2021.

Bivand, R. S., Pebesma, E., and Gomez-Rubio, V.: Applied spatial data analysis with R, Second edition, Springer, NY, https://asdar-book.org/, 2013.

Bray, P. J., Blockley, S. P., Coope, G. R., Dadswell, L. F., Elias, S. A., Lowe, J. J., and Pollard, A. M.: Refining mutual climatic range (MCR) quantitative estimates of palaeotemperature using ubiquity analysis, Quaternary Science Reviews, 25, 1865–1876, https://doi.org/10.1016/j.quascirev.2006.01.023, 2006.

Castañeda, I. S., Caley, T., Dupont, L. M., Kim, J.-H., Malaizé, B., and Schouten, S.: Middle to Late Pleistocene vegetation and climate change in subtropical southern East Africa, Earth and Planetary Science Letters, 450, 306–316, https://doi.org/10.1016/j.epsl.2016.06.049, 2016.

Chase, B. M., Boom, A., Carr, A. S., Carré, M., Chevalier, M., Meadows, M. E., Pedro, J. B., Stager, J. C., and Reimer, P. J.: Evolving southwest African response to abrupt deglacial North Atlantic climate change events, Quaternary Science Reviews, 121, 132–136, https://doi.org/10.1016/j.quascirev.2015.05.023, 2015a.

Chase, B. M., Lim, S., Chevalier, M., Boom, A., Carr, A. S., Meadows, M. E., and Reimer, P. J.: Influence of tropical easterlies in the southwestern Cape of Africa during the Holocene, Quaternary Science Reviews, 107, 138–148, 2015b.

Chevalier, M.: Enabling possibilities to quantify past climate from fossil assemblages at a global scale, Global and Planetary Change, 175, 27–35, https://doi.org/10.1016/j.gloplacha.2019.01.016, 2019.

Chevalier, M.: GBIF database for CREST, https://doi.org/10.6084/m9.figshare.6743207, 2020.

Chevalier, M. and Chase, B. M.: Southeast African records reveal a coherent shift from high- to low-latitude forcing mechanisms along the east African margin across last glacial–interglacial transition, Quaternary Science Reviews, 125, 117–130, https://doi.org/10.1016/j.quascirev.2015.07.009, 2015.

Chevalier, M. and Chase, B. M.: Determining the drivers of long-term aridity variability: a southern African case study, Journal of Quaternary Science, 31, 143–151, https://doi.org/10.1002/jqs.2850, 2016.

Chevalier, M., Cheddadi, R., and Chase, B. M.: CREST (Climate REconstruction SofTware): a probability density function (PDF)-based quantitative climate reconstruction method, Climate of the Past, 10, 2081–2098, https://doi.org/10.5194/cp-10-2081-2014, 2014.

Chevalier, M., Chase, B. M., Quick, L. J., Dupont, L. M., and Johnson, T. C.: PANGAEA dataset associated with "Temperature change in subtropical southeastern Africa during the past 790,000 years", https://doi.org/10.1594/PANGAEA.915923, 2020a.

Chevalier, M., Davis, B. A. S., Heiri, O., Seppä, H., Chase, B. M., Gajewski, K., Lacourse, T., Telford, R. J., Finsinger, W., Guiot, J., Kühl, N., Maezumi, S. Y., Tipton, J. R., Carter, V. A., Brussel, T., Phelps, L. N., Dawson, A., Zanon, M., Vallé, F., Nolan, C., Mauri, A., de Vernal, A., Izumi, K., Holmström, L., Marsicek, J., Goring, S. J., Sommer, P. S., Chaput, M., and Kupriyanov, D.: Pollen-based climate reconstruction techniques for late Quaternary studies, Earth-Science Reviews, 210, 103 384, https://doi.org/10.1016/j.earscirev.2020.103384, 2020b.

Chevalier, M., Chase, B. M., Quick, L. J., Dupont, L. M., and Johnson, T. C.: Temperature change in subtropical southeastern Africa during the past 790,000 yr, Geology, 49, 71–75, https://doi.org/10.1130/G47841.1, 2021a.

Chevalier, M., Chase, B. M., Quick, L. J., and Scott, L.: An atlas of southern African pollen types and their climatic affinities, Palaeoecology of Africa, 35, 239–258, https://www.taylorfrancis.com/books/9781003162766/chapters/10.1201/9781003162766-15, 2021b.

Cordova, C. E., Scott, L., Chase, B. M., and Chevalier, M.: Late Pleistocene-Holocene vegetation and climate change in the Middle Kalahari, Lake Ngami, Botswana, Quaternary Science Reviews, 171, 199–215, https://doi.org/10.1016/j.quascirev.2017.06.036, 2017.

Costello, M. J., Tsai, P., Wong, P. S., Cheung, A. K. L., Basher, Z., and Chaudhary, C.: Marine biogeographic realms and species endemicity, Nature Communications, 8, 1–9, https://doi.org/10.1038/s41467-017-01121-2, 2017.

Dupont, L. M., Caley, T., Kim, J.-H., Castañeda, I. S., Malaizé, B., and Giraudeau, J.: Glacial-interglacial vegetation dynamics in South Eastern Africa coupled to sea surface temperature variations in the Western Indian Ocean, Climate of the Past, 7, 1209–1224, https://doi.org/10.5194/cp-7-1209-2011, 2011.

Dupont, L. M., Caley, T., and Castañeda, I. S.: Effects of atmospheric CO2 variability of the past 800 kyr on the biomes of southeast Africa, Climate of the Past, 15, 1083–1097, https://doi.org/10.5194/cp-15-1083-2019, 2019.

Fick, S. E. and Hijmans, R. J.: WorldClim 2: new 1-km spatial resolution climate surfaces for global land areas, International Journal of Climatology, 37, 4302–4315, https://doi.org/10.1002/joc.5086, 2017.

Garcia, H. E., Weathers, K., Paver, C., Smolyar, I., Boyer, T., Locarnini, R., Zweng, M., Mishonov, A., Baranova, O., Seidov, D., and Reagan, J.: World Ocean Atlas 2018, Volume 3: Dissolved Oxygen, Apparent Oxygen Utilization, and Dissolved Oxygen Saturation., NOAA Atlas NESDIS 83, p. 38pp, 2019a.

Garcia, H. E., Weathers, K., Paver, C., Smolyar, I., Boyer, T., Locarnini, R., Zweng, M., Mishonov, A., Baranova, O., Seidov, D., Reagan, J., and Others: World Ocean Atlas 2018. Vol. 4: Dissolved Inorganic Nutrients (phosphate, nitrate and nitrate+nitrite, silicate), NOAA Atlas NESDIS 84, p. 35pp, 2019b.

Garnier, Simon, Ross, Noam, Rudis, Robert, Camargo, Pedro, A., Sciaini, Marco, Scherer, and Cédric: viridis - Colorblind-Friendly Color Maps for R, https://doi.org/10.5281/zenodo.4679424, r package version 0.6.1, 2021.

GBIF: GBIF: Global Biodiversity Information Facility, https://www.gbif.org, 2018.

GBIF: Beetles occurrence data downloaded on September 24th, 2020, https://doi.org/10.15468/dl.nteruy, 2020a.

GBIF: Chironomids occurrence data downloaded on September 24th, 2020, https://doi.org/10.15468/dl.jv3wsh, 2020b.

GBIF: Diatoms occurrence data downloaded on September 24th, 2020, https://doi.org/10.15468/dl.vfr257, 2020c.

GBIF: Foraminifera occurrence data downloaded on September 24th, 2020, https://doi.org/10.15468/dl.692yg6, 2020d.

GBIF: Rodentia occurrence data downloaded on September 24th, 2020, https://doi.org/10.15468/dl.fscw6q, 2020e.

GBIF: Cycadopsidae occurrence data downloaded on September 24th, 2020, https://doi.org/10.15468/dl.sfjzxu, 2020f.

GBIF: Magnoliopsida occurrence data downloaded on September 24th, 2020, https://doi.org/10.15468/dl.ra49dt, 2020g.

GBIF: Anthocerotopsida occurrence data downloaded on September 24th, 2020, https://doi.org/10.15468/dl.t9zenf, 2020h.

GBIF: Gingkoopsidae occurrence data downloaded on September 24th, 2020, https://doi.org/10.15468/dl.da9wz8, 2020i.

GBIF: Gnetopsidae occurrence data downloaded on September 24th, 2020, https://doi.org/10.15468/dl.h2kjnc, 2020j.

GBIF: Liliopsida occurrence data downloaded on September 24th, 2020, https://doi.org/10.15468/dl.axv3yd, 2020k.

GBIF: Lycopodiopsida occurrence data downloaded on September 24th, 2020, https://doi.org/10.15468/dl.ydhyhz, 2020l.

GBIF: Pinopsidae occurrence data downloaded on September 24th, 2020, https://doi.org/10.15468/dl.x2r7pa, 2020m.

GBIF: Polypodiopsida occurrence data downloaded on September 24th, 2020, https://doi.org/10.15468/dl.87tbp6, 2020n.

GBIF: Bryophyta occurrence data downloaded on August 2nd, 2021, https://doi.org/10.15468/DL.WD527G, 2021a.

GBIF: Marchantiophyta occurrence data downloaded on August 2nd, 2021, https://doi.org/10.15468/DL.M2SSE4, 2021b.

Gibson, M. E., McCoy, J., O'Keefe, J. M. K., Nuñez Otaño, N. B., Warny, S., and Pound, M. J.: Reconstructing terrestrial paleoclimates: a comparison of the Co-existence Approach, Bayesian and probability reconstruction techniques using the UK Neogene, Paleoceanography and Paleoclimatology, https://doi.org/10.1029/2021PA004358, 2022.

Hijmans, R. J.: raster: Geographic Data Analysis and Modeling, https://CRAN.R-project.org/package=raster, r package version 3.4-13, 2021.

Hui, Z., Zhou, X., Chevalier, M., Wei, X., Pan, Y., and Chen, Y.: Miocene East Asia summer monsoon precipitation variability and its possible driving forces, Palaeogeography, Palaeoclimatology, Palaeoecology, 581, 110 609, https://doi.org/10.1016/j.palaeo.2021.110609, 2021.

Hutson, W. H.: Application of transfer functions to Indian Ocean planktonic Foraminifera, Quaternary Research, 9, 87–112, https://doi.org/10.1016/0033-5894(78)90084-4, 1978.

Juggins, S.: Quantitative reconstructions in palaeolimnology: new paradigm or sick science?, Quaternary Science Reviews, 64, 20–32, https://doi.org/10.1016/j.quascirev.2012.12.014, 2013.

Kühl, N., Gebhardt, C., Litt, T., and Hense, A.: Probability Density Functions as Botanical-Climatological Transfer Functions for Climate Reconstruction, Quaternary Research, 58, 381–392, https://doi.org/10.1006/qres.2002.2380, 2002.

Lim, S., Chase, B. M., Chevalier, M., and Reimer, P. J.: 50,000 years of climate in the Namib Desert, Pella, South Africa, Palaeogeography, Palaeoclimatology, Palaeoecology, 451, 197–209, https://doi.org/10.1016/j.palaeo.2016.03.001, 2016.

Lincoln, M.: clipr: Read and Write from the System Clipboard, https://CRAN.R-project.org/package=clipr, r package version 0.7.1, 2020.

Locarnini, R., Mishonov, A., Baranova, O., Boyer, T., Zweng, M., Garcia, H. E., Reagan, J., Seidov, D., Weathers, K., Paver, C., Smolyar, I., and Others: World ocean atlas 2018, volume 1: Temperature, NOAA Atlas NESDIS 81, p. 52pp, 2019.

Myers, N., Mittermeier, R. A., Mittermeier, C. G., da Fonseca, G. A. B., and Kent, J.: Biodiversity hotspots for conservation priorities, Nature, 403, 853–858, https://doi.org/10.1038/35002501, 2000.

Olson, D. M., Dinerstein, E., Wikramanayake, E. D., Burgess, N. D., Powell, G. V. N., Underwood, E. C., D'amico, J. A., Itoua, I., Strand, H. E., Morrison, J. C., Loucks, C. J., Allnutt, T. F., Ricketts, T. H., Kura, Y., Lamoreux, J. F., Wettengel, W. W., Hedao, P., and Kassem, K. R.: Terrestrial Ecoregions of the World: A New Map of Life on Earth: A new global map of terrestrial ecoregions provides an innovative tool for conserving biodiversity, BioScience, 51, 933, https://doi.org/10.1641/0006-3568(2001)051[0933:TEOTWA]2.0.CO;2, 2001.

Overpeck, J. T., Webb III, T., and Prentice, I. C.: Quantitative interpretation of fossil pollen spectra: Dissimilarity coefficients and the method of modern analogs, Quaternary Research, 23, 87–108, https://doi.org/10.1016/0033-5894(85)90074-2, 1985.

Pebesma, E. J. and Bivand, R. S.: Classes and methods for spatial data in R, R News, 5, 9–13, https://CRAN.R-project.org/doc/Rnews/, 2005.

Quick, L. J., Chase, B. M., Carr, A. S., Chevalier, M., Grobler, B. A., and Meadows, M. E.: A 25,000 year record of climate and vegetation change from the southwestern Cape coast, South Africa, Quaternary Research, pp. 1–18, https://doi.org/10.1017/qua.2021.31, 2021.

R Core Team: R: A Language and Environment for Statistical Computing, R Foundation for Statistical Computing, Vienna, Austria, https://www.R-project.org/, 2020.

R Special Interest Group on Databases (R-SIG-DB), Wickham, H., and Müller, K.: DBI: R Database Interface, https://CRAN.R-project.org/package=DBI, r package version 1.1.1, 2021.

Reynolds, R. W., Smith, T. M., Liu, C., Chelton, D. B., Casey, K. S., and Schlax, M. G.: Daily high-resolution-blended analyses for sea surface temperature, Journal of Climate, 20, 5473–5496, https://doi.org/10.1175/2007JCLI1824.1, 2007.

Schauberger, P. and Walker, A.: openxlsx: Read, Write and Edit xlsx Files, https://CRAN.R-project.org/package=openxlsx, r package version 4.2.3, 2020.

Soetaert, K.: plot3D: Plotting Multi-Dimensional Data, https://CRAN.R-project.org/package=plot3D, r package version 1.4, 2021.

ter Braak, C. J. F. and van Dame, H.: Inferring pH from diatoms: a comparison of old and new calibration methods, Hydrobiologia, 178, 209–223, https://doi.org/10.1007/BF00006028, 1989.

ter Braak, C. J. F., Juggins, S., Birks, H. J. B., and van der Voet, H.: Weighted averaging partial least squares regression (WA-PLS): Definition and comparison with other methods for species-environment calibration, Multivariate Environmental Statistics, pp. 525–560, https://doi.org/10.1007/BF00028046, 1993.

Valavi, R., Guillera-Arroita, G., Lahoz-Monfort, J. J., and Elith, J.: Predictive performance of presence-only species distribution models: a benchmark study with reproducible code, Ecological Monographs, 0, 1–27, https://doi.org/10.1002/ecm.1486, 2021.

Wickham, H.: The Split-Apply-Combine Strategy for Data Analysis, Journal of Statistical Software, 40, 1–29, http://www.jstatsoft.org/v40/i01/, 2011.

Wickham, H.: stringr: Simple, Consistent Wrappers for Common String Operations, https://CRAN.R-project.org/package=stringr, r package version 1.4.0, 2019.

Wickham, H. and Hesselberth, J.: pkgdown: Make Static HTML Documentation for a Package, https://CRAN.R-project.org/package=pkgdown, r package version 1.6.1, 2020.

Wickham, H. and Seidel, D.: scales: Scale Functions for Visualization, https://CRAN.R-project.org/package=scales, r package version 1.1.1, 2020.

Wickham, H., Hester, J., and Chang, W.: devtools: Tools to Make Developing R Packages Easier, https://CRAN.R-project.org/package=devtools, r package version 2.3.2, 2020.

Wickham, H., Ooms, J., and Müller, K.: RPostgres: 'Rcpp' Interface to 'PostgreSQL', https://CRAN.R-project.org/package=RPostgres, r package version 1.3.3, 2021.

Wright, K.: pals: Color Palettes, Colormaps, and Tools to Evaluate Them, https://CRAN.R-project.org/package=pals, r package version 1.7, 2021.

Yi, S., Jun, C. P., nam Jo, K., Lee, H., Kim, M. S., Lee, S. D., Cao, X., and Lim, J.: Asynchronous multi-decadal time-scale series of biotic and abiotic responses to precipitation during the last 1300 years, Scientific Reports, 10, 1–10, https://doi.org/10.1038/s41598-020-74994-x, 2020.

Zomer, R. J., Trabucco, A., Bossio, D. A., and Verchot, L. V.: Climate change mitigation: A spatial analysis of global land suitability for clean development mechanism afforestation and reforestation, Agriculture, Ecosystems & Environment, 126, 67–80, https://doi.org/10.1016/j.agee.2008.01.014, 2008.

Zweng, M., Seidov, D., Boyer, T., Locarnini, R., Garcia, H. E., Mishonov, A., Baranova, O., Weathers, K., Paver, C., Smolyar, I., and Others: World Ocean Atlas 2018, Volume 2: Salinity, NOAA Atlas NESDIS 82, p. 50pp, 2018.